RESEARCH FRONT

Review

CSIRO PUBLISHING

Aust. J. Chem. **2009**, *62*, 762–785

www.publish.csiro.au/journals/ajc

Polymer/Carbon Nanotube Composites

Caroline McClory,[A] *Seow Jecg Chin*,[A] *and Tony McNally*[A,B]

[A]School of Mechanical and Aerospace Engineering, Queen's University Belfast, Belfast BT9 5AH, UK.

[B]Corresponding author. Email: t.mcnally@qub.ac.uk

The unique geometry and extraordinary mechanical, electrical, and thermal conductivity properties of carbon nanotubes (CNTs) make them ideal candidates as functional fillers for polymeric materials. In this paper we review the advances in both thermoset and thermoplastic CNT composites. The various processing methods used in polymer/CNT composite preparation; solution mixing, in-situ polymerization, electrospinning, and melt blending, are discussed. The role of surface functionalization, including 'grafting to' and 'grafting from' using atom transfer radical polymerization (ATRP), radical addition–fragmentation chain transfer polymerization (RAFT), and ring-opening metathesis polymerization (ROMP) in aiding dispersion of CNTs in polymers and interfacial stress transfer is highlighted. In addition the effect of CNT type, loading, functionality and alignment on electrical and rheological percolation is summarized. We also demonstrate the effectiveness of both Raman spectroscopy and oscillatory plate rheology as tools to characterize the extent of dispersion of CNTs in polymer matrices. We conclude by briefly discussing the potential applications of polymer/CNT composites and highlight the challenges that remain so that the unique properties of CNTs can be optimally translated to polymer matrices.

Manuscript received: 6 March 2009.
Final version: 15 July 2009.

Contents

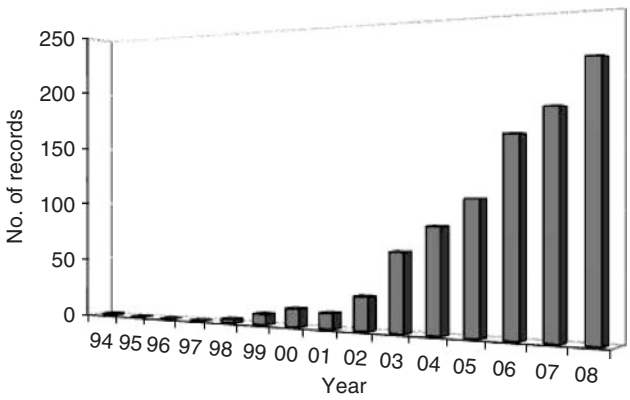

Fig. 1. Articles on polymer/CNT composites that appear in the journal literature.[2]

1. Introduction

Since the identification of multi-walled carbon nanotubes (MWCNTs) in 1991 and the first published report by Ajayan et al. on polymer/carbon nanotube (CNT) composites in 1994,[1] there has been an exponential growth in the number of polymer/CNT composite publications, see Fig. 1.[2] The now well documented unique chemical structure and extraordinary mechanical, electrical, and thermal conductivity properties of CNTs have prompted an incredible research effort over the past decade to uncover the inherent possibilities that lie in using these one-dimensional (1D) tubes as reinforcing filler materials in polymers.

From a historical perspective, it is worth noting that before 1991 there had been several references to CNT-like structures, including 'carbon tubes'[3] and 'hollow carbon fibres'.[4] Moreover, it has been proposed that when Thomas Edison was developing the light bulb *c*. 1880 using carbonized bamboo filaments, such carbon structures may have been produced.[5] However, the first large-scale use of CNTs is in composite technology, initially where polymers have been the matrix material, but increasingly with metals and ceramics. A limited number of reviews on polymer/CNT composites have been published to date,[6–16] with most focusing on specific topics, such as the use of CNTs and their composites as sensors and actuators,[6]

10.1071/CH09131 0004-9425/09/080762

elastomer/CNT composites,[8] and the mechanical properties of CNT composites.[10]

2. Early Studies on Polymer/CNT Composites

CNTs have extraordinary strength, and electrical and thermal conductivity, and continue to fascinate material scientists across the globe because of the numerous technological possibilities that polymer/CNT composites offer.[17–21] The desire within the advanced composite research community is to seek a polymer/CNT composite with physical properties that approach the theoretical maximum values of an individual nanotube. It is well understood that CNTs have modulus values in the order of 1 TPa.[22] The applications for any such enhanced polymeric material are infinite and would also be highly lucrative. Therefore, the interest in the area of polymer/CNT composites is immense and has increased exponentially since 1994 when Ajayan et al. published the first introduction to the area of polymer/nanotube composites.[1] The work was not initially concerned with the fabrication of a new polymer/nanotube composite but instead focussed on the alignment of CNTs by the cutting action of thin slices of a polymer resin embedded with nanotubes. The authors discovered that nanotubes straightened after the cutting process and withstood the breaking force during cutting, which indicated that CNTs are extremely strong, flexible nanofibres with exceptional mechanical properties. This was contrary to other work published at the time by Ruoff et al. that suggested small nanotubes could be flattened by weak van der Waals forces between individual tubes.[23] It was now possible to organize nanotubes into micrometer-sized arrays and the authors suggested that the removal of the surrounding resin by an etching process would leave the remaining arrangement of single nanotubes available for the fabrication of novel 1D nanodevices for mechanical and transport testing. These properties could now be measured and related to individual tube size and helicity. This work demonstrated that it was possible to use polymers as a medium to study CNTs in much greater detail than ever before and paved the way for subsequent studies on the individual properties of nanotubes. Several further studies are important milestones in the development of polymer–nanotube composites. Studies lead by Wagner in 1998 used nanotube-filled polymeric films to observe single nanotube fragmentation under tensile stresses.[24] The CNTs used were multi-walled, produced by an arc-discharge process, and sonicated in ethanol to aid dispersion. A urethane/diacrylate oligomer was the matrix material and was simply spread over the dispersed nanotubes on a glass surface. The final nanotube composite was formed by an in-situ polymerization process using UV light to cure the liquid polymer–nanotube mixture. A 200 μm amorphous film was produced and cut into strips for mechanical testing. Thin microtomed sections (~70 nm) of deformed and non-deformed material were inspected by transmission electron microscopy (TEM). A progressive nanotube fragmentation process was observed in the stressed samples. The tensile stresses generated by polymer deformation were transmitted to the nanotube during the fragmentation experiment.[24] A nanotube–matrix interfacial shear stress mechanism occurring at the molecular level was responsible for the transfer of shear forces from the polymer matrix to the nanotubes. A simplified version of the Kelly–Tyson model[25] shown in Eqn 1 was used to indicate that the fibre–matrix stress transfer ability was as much as 500 MPa, which was at least one order of magnitude larger than that of conventional fibre-based composites at that time. The interfacial shear stress, τ_{NT}, can be determined from:

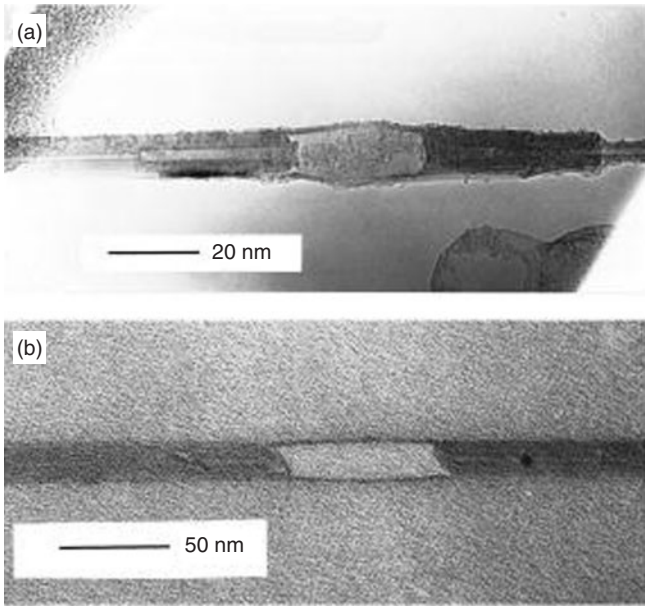

Fig. 2. Examples of telescopic rupture of a MWCNT in a polymer film. Note the intact wall–polymer interface, contrasting with the longitudinal rupture in shear of the internal wall structure. (Reproduced with permission from AIP to reproduce from ref. [24].)

$$\tau_{NT} = \frac{\sigma_{NT}(L_c)}{2(L_c/D_{NT})}\left(1 - \frac{d_{NT}^2}{D_{NT}^2}\right), \quad (1)$$

where σ_{NT}, L_c, d, and D are the failure stress, critical length, and inner and outer diameter of the CNTs, respectively. 'Telescopic' rupture of the MWCNTs was observed within the polymer film where the outer wall of the nanotube in contact with the matrix remained intact while the internal walls had ruptured under the applied stress, see Fig. 2.

In more recent reports this 'sliding' or 'telescopic' mechanism has been used to describe the method of failure of multi-walled tubes within a polymer matrix.[26] Wagner et al. suggested the likely reactivity of CNTs to polymer chains that contained double bonds during the UV-curing process as being responsible for the high mechanical strength of this polymer–nanotube interface. This, coupled with end-cap defects, is proposed as a mechanism of interfacial reinforcement of this polymer/nanotube composite. This study into the fragmentation behaviour of MWCNTs was ground-breaking, and identified, in part, issues surrounding the matrix–nanotube behaviour that today are still being answered.[24]

An epoxy resin/MWCNT composite was prepared using a similar method as described in ref. [24] by Lourie et al.[27] Amorphous films ~200–300 μm thick were produced and the effect of the compressive forces applied to nanotubes during the polymerization process were observed by TEM. The nanotubes seemed to bend and loop under compression with kinks observed on the inside bend of the tubes. Using experimentation and the theory of elastic stability, this work provided the first estimation of the compressive strength of CNTs, ~60 GPa. It was approximated at more than two orders of magnitude greater than that previously reported for any other fibre. The nanotubes were found to collapse under compressive stress because of the disintegration and progressive fragmentation of tubes.[27] This has proven to be one of the earliest insights into the compressive behaviour of

CNTs embedded within a polymer medium. Subsequent work by Schadler et al., again in 1998, probed further into the mechanical behaviour of epoxy resin/CNT composites by studying the load transfer mechanism from the matrix to the nanotubes in both tension and compression.[28] A low loading level of 5 wt-% nanotubes were dispersed with the aid of an ultrasonic probe in the epoxy resin before curing with a triethylene tetraamine hardener. Observations by scanning electron microscopy (SEM) revealed good dispersion of nanotube agglomerates but poor distribution throughout the matrix. Load transfer and the interfacial shear stress between matrix and nanotube were the focal point of the letter and three mechanisms of load transfer were proposed. The first was the micromechanical interlocking of a CNT within a polymer material. The authors suggest that the difficulty in pulling a nanotube out of its place within a polymer matrix adds to the interfacial shear stress between materials. Second, there may be chemical bonding between nanotubes and the polymer. The direct covalent attachment of CNTs to the polymer matrix has in recent years proven to be very desirable in the formation of high strength, mechanically enhanced composite materials. The third and final mechanism of load transfer proposed by Schadler et al. is naturally occurring weak van der Waals bonding between the nanotube and matrix.[28] An interesting point to note in this work is the unusual behaviour that nanotubes exhibit when the comparison is made between their stress response under tension and compression. Significant differences were noted in the Raman response of the G′ band to the composite when under each mode of stress. A Raman peak shift is attributable to the changes in the inter-atomic distances within a material as it is deformed. The larger the Raman peak shift, the larger is the strain carried by the nanotubes. The positive, smaller Raman peak shift when in tension is a result of the low load transfer behaviour of the nanotubes under tensile stress. In contrast, when in compression, the Raman response is negative and much larger, which indicates that the nanotubes carry a much greater strain in compression. It was proposed that during load transfer to multi-walled nanotubes, only the outer layers are stressed under tension whereas all the layers respond under compression.[28] In this work both the tensile and compressive modulii of the nanocomposites were compared with the pristine epoxy resin. The tensile modulus improved from 3.1 to 3.71 GPa, and the compression modulus improved from 3.63 to 4.5 GPa on addition of 5 wt-% CNTs. The average and maximum values of the compression modulus are larger than the tensile values.

Many of the early studies on polymer/nanotube composites focussed mainly on the mechanical properties of epoxy resins and other thermosets. The impetus was clear from the early 1990s that if CNTs were as strong as theoretically predicted, they could provide scientists with a novel reinforcing phase for composite materials. Although the mechanical properties of CNTs in 1998 were very attractive, the reality of exploiting these in a macroscopic composite was unclear.[29] Work undertaken by Wang et al. showed a more immediate application that would take advantage of the electronic properties of nanotubes in the fabrication of flat panel displays and nanometer-scale electronic devices.[17]

Curran et al. in 1998 reported the first physical doping using MWCNTs in a conjugated luminescent polymer, poly(*m*-phenylenevinylene-*co*-2,5-dioctoxy-*p*-phenylene vinylene) (PmPV) in a polymer/nanotube composite.[18] The aim of the study was to produce an organic light-emitting diode (LED) aided by the incorporation of MWCNTs in a conjugated polymer. This had been a difficult task in the past as polymers for use in LEDs must be un-doped and possess a high quantum yield of photoluminescence. As most un-doped polymers are electrical insulators, a high 'turn on' field must be used in order to achieve the levels of photoluminescence required for this application, and the result is device breakdown because of thermal effects.[18] Increasing the conductivity of the conjugated polymer was, therefore, an attractive option. Arc discharge-produced MWCNTs were sonicated in toluene along with the dissolved polymer. The group were successful in increasing the electrical conductivity of PmPV by eight orders of magnitude upon the addition of a 0.35 mass fraction of MWCNTs in PmPV from 10^{-10} to 10^{-2} S m^{-1}. The authors claimed the uniform dispersion of nanotubes, and the observation of polymer inside the nanotubes by TEM studies provided evidence for excellent polymer–nanotube interfacial interactions and thus improved mechanical properties of PmPV. The usual degradation of the conjugated polymer by electrical and/or optical thermal effects was avoided by the action of the nanotubes as thermal heat sinks. This study was one of the first to prove how it was possible to use organic materials as active components in optoelectronic applications. Just a year later in 1999, Shaffer and Windle commented on the status of CNT composites at that time.[29] Their work described the fabrication and subsequent characterization of CNT/poly(vinyl alcohol) (PVA) composite films. They described a processing route for PVA/nanotube composites by means of forming a stable colloidal intermediate, a method applicable to the fabrication of other polymer/nanotube systems. PVA is water soluble, therefore, aqueous PVA solutions, $[CH_2CH(OH)]_n$ (PVOH) were mixed with a chemically treated, electrostatically stable dispersion of aqueous CNTs. Composite films that varied in thickness from 44 to 53 μm were prepared by a casting method. The nanotubes observed by SEM were thought to be uniformly dispersed, and from thermogravimetric analysis the addition of the nanotubes was found to retard the onset of the thermal degradation of PVA by 80°C for an optimum nanotube loading of 20 wt-%. The authors proposed that this retardation effect was a result of the surface of the CNTs absorbing the free-radicals produced during polymer decomposition. Dynamic mechanical analysis (DMA) of the composites revealed that the nanotubes had a significantly higher stiffening effect above the glass transition temperature (T_g) of the PVOH. Above the T_g, the nanotubes retained the stiffness the constrained polymer chains experienced below the glass transition, and the modulus values increased with nanotube loading. Electrical conductivity measurements were carried out using impedance spectroscopy and a percolation threshold for these composites was achieved between 5 and 10 wt-% nanotube loading. This was significantly higher than the percolation threshold between 0.0225 and 0.04 wt-%, previously reported by Sandler et al. for an untreated catalytically grown CNT-filled epoxy resin.[19] The high percolation threshold reported in the PVOH study is almost certainly a consequence of an adsorbed layer of polymer, which reduces the quality and quantity of electrical contacts between nanotubes.[29]

In summary, for the period spanning 1994–1999 several studies demonstrated that CNTs had the potential to be used in the formation of nanodevices.[1] Furthermore, the fragmentation and telescopic rupture of a single MWCNT was observed and several load transfer mechanisms within polymer/CNT composites proposed.[24,28] Studies were performed on the compressive response of MWCNTs using Raman spectroscopy[27,28] and finally several polymer/CNT composites displayed electrically conductive behaviour.[18,19,29] These initial results, coupled with

the unique individual properties of nanotubes, led to an explosion of research into polymer/CNT composites.

3. Thermosetting Polymer/CNT Composites

3.1. Introduction

In the years following the initial interest in the field of polymer/CNT composites there has been a surge of studies and literature available to researchers. The literature to date has focussed on the methods of dispersion and distribution of the CNTs within the polymer matrix and how interactions of polymer chains and CNTs can be promoted. Melt-mixing,[20,21] solution-casting,[30] and in-situ polymerization[31] have all been employed for CNT/polymer composite synthesis. Nanotube dispersion can be aided by low-impact ball milling,[32] the use of surfactants,[33] ultrasonic vibration,[34,35] and surface functionalization by means of acid[36] or plasma[37] treatments. Most of the literature has reported on thermoplastic/CNT composite materials, including some very recent review articles,[10,38] but to a much lesser extent on thermoset/CNT composites, which is somewhat surprising as thermosets account for 25% of the global market of all natural and synthetic polymeric materials. The majority of thermoset–CNT studies have focussed on epoxy[31] and thermosetting polyimide[35]/CNT composites. The following sections will discuss many of the issues regarding processing variations, dispersive aids and the mechanical, electrical, and thermal behaviour of thermoset/CNT composites.

3.2. Composite Preparation Methods and Dispersion of CNT Phase

As stated previously, the most common thermoset material used in the manufacture of thermosetting polymer/CNT composites is epoxy resin. Epoxy is extensively used in the aerospace, coating, and electronic industries because of its high strength, good chemical resistance, high heat distortion temperature, and adhesive nature.[31] It is, therefore, not surprising that it has been the focus of many interesting studies into the enhancement and preparation of an already versatile polymer by the addition of fillers. There is an abundance of literature on the mechanical[39,40] and electrical[41,42] properties of epoxy/CNT composites, with several studies focusing on the benefits of the functionalization of CNTs before composite synthesis.[43,44] A homogeneous dispersion of nanotubes throughout a matrix and good polymer–nanotube interfacial interactions are crucial factors in achieving enhanced mechanical properties of a composite. Contrary to this, during the insulator-to-conductor transition of a polymer/nanotube composite, the formation of a three-dimensional (3D) network of nanotubes or a system of small nanotube clusters throughout the bulk material is essential to improve electrical conductivity. Therefore, careful preparation of a polymer/CNT composite may assist the dispersion of nanotube agglomerates and the manipulation of nanotube behaviour in a polymer matrix. A good preparation methodology is, therefore, an integral part of the process and can be adapted to achieve good mechanical properties, improved electrical behaviour, or both. Sandler et al.[19] used a method of dispersion previously described for the preparation of epoxy resin using carbon black as the filler of choice.[45] An epoxy based on bisphenol-A resin was cured by the addition of an aromatic hardener. Prior to curing, several stages were used to add the untreated, catalytically grown MWCNTs to the epoxy while aiding dispersion. The entangled CNTs (length 5–10 μm and ~10 nm outer diameter) were initially dispersed in ethanol in an ultrasonic bath for 1 h. This solution was then mechanically stirred into the epoxy prepolymer at 2000 rpm for 1 h. After solvent evaporation (80°C, 1 h vacuum oven), the hardener was added, and the mixture was stirred and cast into moulds. It is interesting to note that during the stirring process the viscosity of the suspension was kept low by raising the temperature to 80°C using an oil-silicone bath. This was necessary at filler weight fractions above 1 wt-% as the nanotubes strongly increased the viscosity of the resin. Contrary to conventional understanding, lowering the viscosity of a liquid is more effective in aiding nanotube dispersion than a highly viscous system. Although the mechanical shear forces acting on a liquid are increased in a highly viscous fluid, the effective area of dispersion can be localized, for example, at the area close to the tip of an ultrasonic horn or the area surrounding a stirring disc, which results in poor overall dispersion. An optimum level of resin viscosity must be reached, as the viscosity of the fluid must not be low enough to allow the nanotubes to re-aggregate uncontrollably by van der Waals attractions before they are properly dispersed. A low viscosity fluid is thought to increase the surface wetting of the nanotubes and polymer chains. In assessment of the state of the dispersion of nanotubes in the epoxy composite, the authors admit it is not possible to disperse all the nanotube bundles by the chosen processing method, although ultrasound and intense mechanical stirring seem to have facilitated a satisfactory degree of mixing. A 3D conductive path of nanotubes and nanotube aggregates was formed on addition of the hardener, and an electrical percolation threshold of between 0.0225 and 0.04 wt-% achieved with this level of nanotube dispersion.

Controlled re-aggregation of well-dispersed CNTs in the same epoxy resin in order to form a 'touching' 3D network of nanotubes was the focus of further work by the same research group.[41] Aligned MWCNTs, produced by an injection chemical vapour deposition (CVD) method (length 17 ± 3 μm and ~50 nm outer diameter) achieved a percolation threshold (0.0025 wt-%, see Fig. 3) one order of magnitude lower than what was previously reported for entangled CNTs in the same epoxy resin.[19] This is attributed to the purity and geometry of the aligned nanotubes and also the refinement of the processing methodology used. A sequence of increasing and reducing the temperature of the epoxy resin was used at different stages of the dispersion process to optimize final electrical properties of the composite. No solvent was used in this instance and instead the nanotubes were mechanically sheared into the epoxy resin precursor at room temperature and 2000 rpm for 1 h. Next, dry ice was used to lower the temperature of the mixture and further stirring was carried out for 1 h at 2000 rpm. The lower temperature raises the viscosity of the liquid (as the aligned nanotubes had no effect on viscosity), therefore, increasing the shear forces acting on the already dispersed nanotubes in the epoxy. The temperature is then allowed to equilibrate at 80°C for 10 min at 0 rpm. The final stage, which involved the addition of hardener, was optimized to enhance the nanotube re-agglomeration process and homogeneous dispersion of hardener. At such low nanotube loadings, steps must be taken in order to promote the 3D network of touching nanotubes necessary for insulator–conductor transition (percolation). The hardener is stirred into the resin–nanotube suspension at 500 rpm for 1 min and 50 rpm for 4 min. On addition of the hardener, the dispersed nanotubes quickly re-aggregate as the polymer begins to form cross-links. These low stirring rates promote the growth of a 3D nanotube network by mobilizing the nanotubes, which allows them to overcome the repulsive barrier between particles.[19] For composites with high nanotube loading it was possible to examine

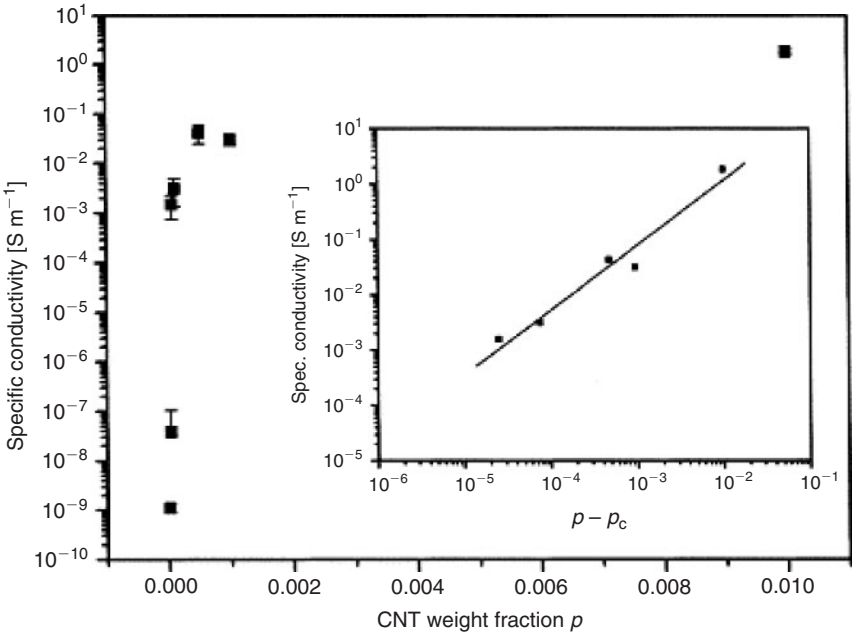

Fig. 3. Semi-log plot of the specific composite conductivity as a function of CNT weight fraction p. The insert shows a log–log plot of the conductivity as a function of $p - p_c$ with an exponent t of 1.2; the critical weight concentration $p_c = 0.0025$ wt-%. (Reproduced with permission from Elsevier to reproduce from ref. [41].)

the formation of small local aggregates by optical microscopy. At a nanotube loading of 0.0025 wt-%, it was possible to see the nanotube aggregates with the naked eye. Above this loading, macroscopic networks are visible on the millimetre scale. SEM images show the transition from a dispersed nanotube state at 0.001 wt-% to small clusters that occur at 0.0025 wt-%. This clustering of nanotubes evenly distributed across the sample leads to the equivalent CNT percolation threshold at this nanotube loading.

In a study by Martin et al., the processing stages in the production of epoxy-aligned MWCNT using the same epoxy material described in refs [19] and [41] were varied.[42] Separate batches were processed, each varying one of three parameters: temperature on addition of hardener, stirring rate on addition of hardener, and cure temperature. All samples contained 0.01 wt-% aligned MWCNTs synthesized by an injection CVD process. Varying the temperature at which the hardener was added revealed the importance of this stage and the temperature dependence of the agglomeration process. At room temperature no agglomeration occurred on addition of the hardener, which resulted in a composite that exhibited insulating behaviour. The authors suggest that the nanotube clusters created during the addition of the hardener at elevated temperatures agglomerated during the curing process to form a conductive network, samples of which exhibit purely ohmic behaviour as measured using alternating current (AC) impedance spectroscopy. Furthermore, the stirring rate used during hardener addition promotes the relative nanotube clustering and the agglomeration required for network formation. The nanotubes require an elevated temperature and an optimum stirring speed to encourage local nanotube clustering. Too high a speed will simply re-disperse the nanotubes, which results in insulating behaviour after curing. The slow stirring rate gives the nanotubes sufficient kinetic energy to overcome the repulsive forces that prevent them from coming out of a stable dispersion to reform small clusters and thus network formation. During an experiment to determine surface charging of the nanotubes in the initial dispersed state, a drop of the nanotube–epoxy dispersion was placed between two gold sputtered electrodes. The application of a direct current (DC) field led to a collection of nanotubes at the anode, as the negative surface charge stabilized the nanotube dispersion. The stability of the initially well-dispersed epoxy precursor/nanotube mixture can be attributed to electrostatic stabilization,[42] which is also a recognized phenomenon in colloidal dispersions[46] and has previously been observed for epoxy/carbon black composites.[47]

The final curing temperature of the resin can also encourage nanotubes to cluster. A high cure temperature lowers the resin viscosity to give the nanotubes more mobility within the curing material. During the same study,[42] the percolation threshold (wt-%) was plotted as a function of aspect ratio for three different MWCNT types that were added to the same epoxy material. Standard percolation theory suggests higher aspect ratio tubes should form a 3D touching network of particles at lower loadings than lower aspect ratio tubes. Interestingly, in this study the lowest percolation value is recorded for the nanotubes with the lowest aspect ratio. This is explained by the mobility of the shorter nanotubes ($\times 4$) during the curing stage of the epoxy, the shorter more mobile nanotubes are able to form electrical connections much more quickly. More recently Chen et al. studied the effect of a CNT dispersion on the tribological properties of a CNT-reinforced epoxy resin.[48] The authors reported that the wear resistance of the neat epoxy was improved on addition of 1 wt-% unmodified CNTs and, interestingly, that pretreatment of the CNTs with either nitric acid or silane coupling agent did not yield further enhancement in wear resistance, although this was dependant on the fabrication method used. These reports demonstrate how it is possible to manipulate processing conditions in order to control the end-properties of a polymer/CNT composite. Much of the work undertaken to optimize this process was trial and error. Ultrasound has also been reported to damage and cause tube scission, which reduces the aspect ratio and thus the final properties of the composites.[49,50]

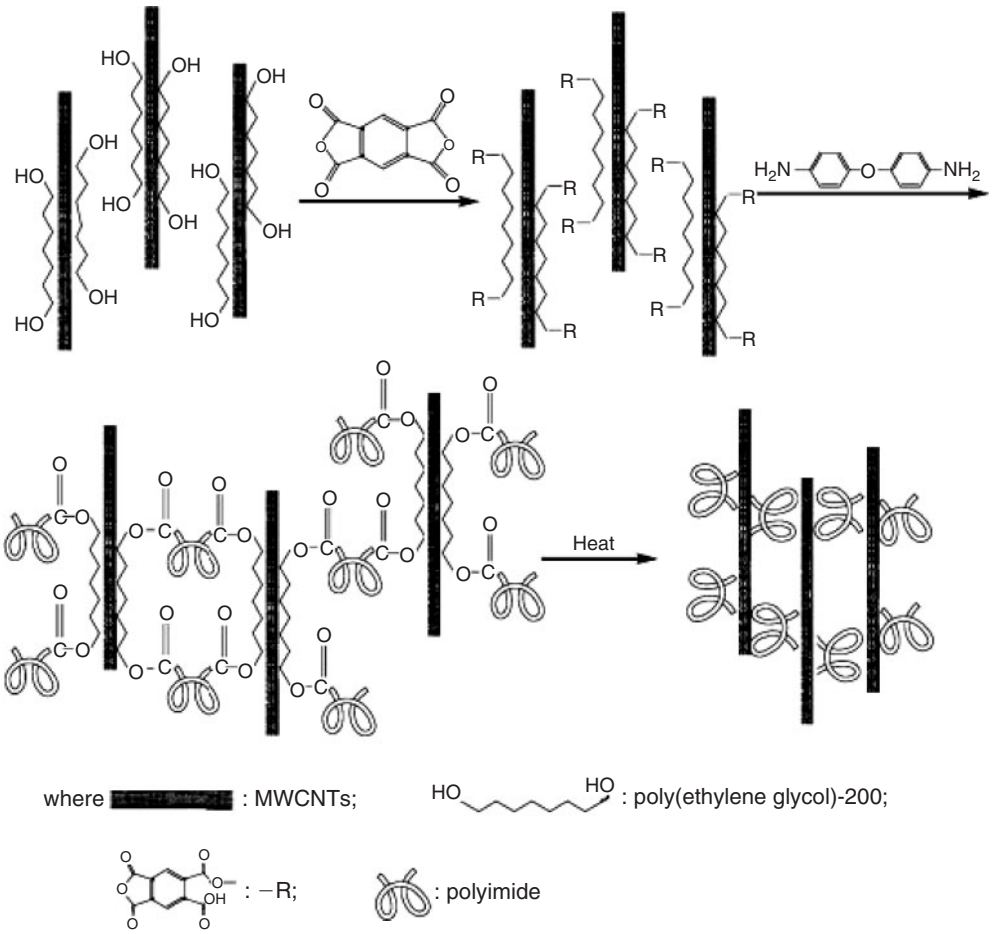

Fig. 4. Illustration of the postulated process of individual MWCNT dispersion in PI with PEG-200 as a dispersing agent. (Reproduced with permission from Wiley Interscience to reproduce from ref. [53].)

A study by Lau et al. involved the dispersion of nanotubes in a solution of *N*,*N*-dimethylformamide (DMF), acetone, and ethanol by ultrasonication before the addition of the epoxy resin.[51] The solvents were removed by controlled evaporation and the epoxy–nanotube suspension cured by the addition of a hardener. Dispersion was improved but the final composite properties were compromised by the residual effect of the solvents and possibly also by the damaging effects of ultrasound on the CNTs.

Yuen et al. reported the preparation and characterization of composites of HNO_3/H_2SO_4-modified MWCNTs, up to a loading of 7 wt-%, with a polyimide.[52] The surface electrical resistivity of the composites was increased by ~9 orders of magnitude with increased MWCNT addition combined with a modest increase in tensile strength and Young's modulus. A further study by Yang et al. described the use of poly(ethylene glycol) (PEG-200) as a processing aid to assist dispersion of MWCNTs in a polyimide at loadings up to 43 wt-%,[53] see Fig. 4. The authors proposed, supported with results from IR, Raman, and UV-vis spectroscopy, that the polymer wraps around the tubes, which suggests strong interfacial interactions as a consequence of π–π stacking between the aromatic rings of the polyimide and the MWCNTs.

3.3. Thermoset Functionalized-MWCNT Composites

An alternate mechanical method of dispersion has been used by Gojny et al. to produce epoxy/double-walled carbon nanotube (DWCNT) composites with enhanced mechanical properties at low nanotube content.[54] A common shear mixing process known as calandering, used extensively in industry for the dispersion of micrometer-scaled particles in cosmetics and paints, was adapted in this study for the dispersion of CNTs. The nanotubes were initially manually sheared into the epoxy resin precursor and then the mixture was added to a three-roll calander. The ceramic rolls were 5 μm apart and rotated at three different speeds of 20, 60, and 180 rpm. This rotating action disperses the nanotubes under high shear forces. The resulting suspension after removal from the calander was stirred for 10 min at room temperature with the hardener material and cured for 24 h at room temperature. Epoxy/non-functionalized and amino-functionalized DWCNT composites were made using this calandering process and a separate set of composites processed using both mechanical stirring and ultrasound. TEM studies indicated that the calandering process resulted in exfoliated agglomerates that measured ≤1.5 μm in diameter, whereas the ultrasonic technique produced samples that contained denser nanotube agglomerates of at least 2 μm in diameter. The authors describe the nanotube agglomerates that remain after the calandering process as 'completely impregnated with epoxy resin' and 'exhibiting an exfoliated structure', although it is quite obvious that the nanotubes are still not completely dispersed and exist only as slightly unravelled entanglements. Mechanical properties of composites made by the calandering process were reported and, in general, very slight improvements were obtained in Young's modulus (6%),

tensile strength (1.5%), and fracture toughness (27%) for a 1 wt-% NH_2-functionalized DWCNT/epoxy composite, although the fracture strain decreased (−7.5%). These improvements were more pronounced than for the non-functionalized epoxy composites because of the dispersion achieved by the amino-functionalized nanotubes. The improved dispersion of the functionalized CNTs was a result of the polar amino groups interacting with the polar epoxy resin.[54] In a further study by Gojny et al. on the dispersion of amino-functionalized CNTs in an epoxy, possible covalent bonding between amino-functional groups and the epoxy resin was suggested but not corroborated with any direct spectroscopic evidence.[55]

Chemical functionalization of the nanotube surface improves the solubility and the dispersion of CNTs within a polymeric material. In a study by Dyke et al. nanotube sidewall functionalization with polar and non-polar aryldiazonium salts was performed in an attempt to separate nanotubes by helicity, either metallic or semiconducting, and resulted in modest levels of success.[56] Furthermore, functionalized nanotubes can provide bonding sites to the polymer matrix so that the load can be transferred to the nanotubes under stress conditions to prevent separation between the polymer surfaces and nanotubes.[55] It is possible to achieve the addition of more than one functional group to a single nanotube as either the end-cap or the sidewall of a nanotube can be modified. The end-caps of a nanotube can be opened under oxidizing conditions and terminated with oxygenated functionalities such as carboxy, carbonyl, and hydroxy groups.[43] In addition to this, a study by Hamon et al. reported that the sidewalls of a nanotube tended to experience chemical attack during oxidative work-up.[57] End-cap functionalization of CNTs is more favourable than sidewall functionalization as it has been demonstrated that the sidewall attachment of functional groups disrupts the electronic structure of single-walled carbon nanotubes (SWCNTs)[58] and hence its electronic conductivity, in addition to some loss of strength.[59] In order to remove metal catalyst impurities from SWCNTs, nitric acid treatment has been shown to efficiently remove 88% of metal impurities while simultaneously introducing carboxy, carbonyl, and hydroxy groups.[60] Carboxylic acid groups can be further reacted to create tubes with various chemical functionalities, for example, esterification reactions[61] or the attachment of long alkyl chains by amide formation.[62]

In a study by Zhu and coworkers, SWCNTs were acid-treated using a mixture of sulfuric and nitric acid.[43] Both pristine and carboxylic acid-terminated SWCNTs were placed in a Monel reactor and fluorinated at 150°C for 12 h. The various types of SWCNTs were ultrasonicated in DMF using both an ultrasonic horn and bath and epoxy composites were made using a loading of 1 wt-%. Attenuated total reflectance infrared (ATR-IR) spectra of the fluorinated SWCNTs, acid-treated SWCNTs, and the acid-treated fluorinated SWCNTs revealed that the added carboxylic acid groups remained intact after fluorination. The appearance of a Raman peak at 1301 cm^{-1} indicated that fluorine was covalently attached to the sidewall of the nanotube. The authors used acid treatment and fluorination of SWCNTs to improve their dispersion throughout the epoxy matrix and also to increase their solubility in a solvent previously demonstrated by Shaffer et al. as suitable for CNTs.[58] Optical microscopy of the pristine and functionalized nanotubes in DMF proved the latter was 'visually non-scattering and homogeneously stable' with an average aggregate size of 300 nm compared with the larger 3 μm average aggregate size of the pristine tubes in DMF. Furthermore, SEM micrographs of the 1 wt-% epoxy composites clearly showed improved dispersion of the functionalized nanotubes in the epoxy matrix. Enhanced dispersion allows more of the nanotube surface to be in contact with the polymer matrix, thus a greater number of functional groups are available for direct bonding to the epoxy resin, which results in a more effective load transfer. The SEM images of the fracture surfaces of functionalized nanotubes in the epoxy indicated that breakage of nanotube bundles had occurred instead of nanotube slippage when deformed under tension, which suggests that a good interfacial interaction existed between the CNTs and epoxy chains. The pristine nanotubes experienced more sliding effects, which suggests inadequate load transfer under tension. The observation of good interfacial bonding in the functionalized SWCNT/epoxy composite was corroborated from mechanical testing, which resulted in improvements in both Young's modulus and tensile strength by 30 and 14%, respectively, over the virgin polymer.

The functionalization of CNTs has the obvious advantages of aiding dispersion in a polymer matrix and the promotion of interfacial bonding between nanotube and polymer as outlined earlier. The addition of a chemical species to the sidewall of a CNT not only disrupts its intrinsic electrical conductivity, but the covalent binding of the tube to the polymer also initiates a physical 'wrapping' of the polymer chain to the tube, which creates an insulating layer around the tube and prevents electron mobility through the composite. The improved interfacial bonding and load transfer is very attractive for mechanical applications but detrimental to the electrical conductivity of the material. This phenomenon was demonstrated in two studies carried out by Gojny and coworkers.[55,63] In both studies using the same material, a modified diglycidyl ether of bisphenol A (DGEBA)-based epoxy resin and amine hardener were used. The first study looked at how nanotube type and functionality affects the mechanical properties of epoxy/CNT composites,[55] and the second paper investigated the electrical and thermal conduction mechanisms in the same CNT-filled epoxy materials.[63] Several interesting conclusions were reported, in particular, the improved dispersion of MWCNTs as opposed to DWCNTs was attributed to the smaller specific surface area of the MWCNTs and hence the easier separation of agglomerations.[64] The improved dispersion of the amino-functionalized nanotubes and the possible covalent bonding between amino functional groups and epoxy led to improvements in strength (10%), stiffness (15%), and fracture toughness (43%) at a DWCNT loading of 0.5 wt-%. The enhancement of the mechanical properties of epoxy by the addition of amino-functionalized DWCNTs is a result of the much improved interfacial adhesion between the nanotubes and the epoxy.

Although the presence of functional groups improved the mechanical properties the opposite was obtained for the electrical conductivity of the samples. The composites with the amino-functionalized CNTs exhibit a higher electrical percolation threshold than those with pristine nanotubes.[63] The non-functionalized nanotubes form a percolation threshold below 0.1 wt-%, whereas the amino-functionalized tubes percolate between 0.1 and 0.5 wt-% loading. This can be explained in terms of the functionalization process, as the amino-modified nanotubes used were synthesized using a ball-milling process in ammonia during which tube rupture could have occurred. The resulting shortening of tube length and hence reduced aspect ratio is responsible for the higher percolation threshold. Second, the addition of amino functional groups to the nanotube disturbs its graphitic structure by introducing sp^3 hybridized carbons to the conjugated system. These sp^3-bonded sites are viewed as defects in terms of electron transport through a nanotube, and

the disruption of the conjugated π-electron system reduces the electrical conductivity of the individual nanotube. Finally, the third effect of introducing functional groups to a CNT greatly improves its interfacial adhesion with polymer chains.[55] This can be to such an extent as to entirely wrap the tube with polymer, thus increasing the distance an electron may have to travel to reach a neighbouring tube. The more difficult it is for an electron to tunnel from tube to tube because of this insulating layer of polymer, the more nanotubes are required to form a percolating network, hence the percolation threshold increases.

A recent study by Kim et al. investigated the effect of surface functionalization on the rheological and mechanical properties of epoxy/CNT composites prepared by ultrasonication.[65] The epoxy resin was based on diglycidyl ether derived from bisphenol-A and a modified aromatic amine. In this work, rheological measurements were used in an attempt to examine changes in the extent of dispersion and interfacial bonding affected by nanotube functionalization. Epoxy/CNT composites were made using acid, amine, plasma, and non-treated MWCNTs. After tensile testing, the fracture surfaces were investigated using field-emission scanning electron microscopy (FESEM) and indicated levels of dispersion and mechanisms of sample failure. The untreated nanotubes were poorly dispersed and were pulled out from the epoxy matrix during fracture. Matrix pull-out indicates poor interfacial bonding between nanotube and matrix and usually leads to poor mechanical properties of the composite. The acid-treated nanotubes were dispersed slightly better but also experienced limited pull-out from the epoxy matrix. The amine-treated nanotubes were poorly dispersed but experienced breakage during fracture. The rupture of the tubes signifies enhanced interfacial bonding and good load transfer between the nanotube and polymer matrix, which is ideal for the improvement of composite mechanical properties. Finally the plasma-treated nanotubes achieved good dispersion in the epoxy and also experienced tube rupture on tensile fracture, and the oxygen groups attached to the CNTs during the Ar plasma treatment contributed to good dispersion and strong interfacial bonding.[65] The linear viscoelastic behaviour of the various epoxy/modified CNT composites was investigated and compared with the pristine polymer. The pure epoxy material exhibited purely Newtonian behaviour as the dynamic shear viscosity was independent of frequency. On the addition of the various nanotubes, the dynamic shear viscosity of the epoxy decreased as the test frequency was increased, and at the lowest test frequency (0.1 rad s^{-1}), the functionalized CNT/epoxy composites had a shear viscosity up to five orders of magnitude higher that that of the pure epoxy. This is because of the strong interfacial bonding that exists between the modified surface of the nanotubes and epoxy, but this varied with nanotube type, and the plasma-modified CNT/epoxy material showed the highest shear viscosity at low frequencies.

3.4. Mechanical and Electrical Properties

The use of high modulus, strength, and aspect ratio CNTs for the mechanical reinforcement of polymers has been a subject of numerous studies. Theoretically, reinforcement on the nanometer scale should provide significant enhancements in a combination of stiffness (modulus), strength, and toughness. However, to date, limited improvements in all these properties for both thermoplastic and thermosetting-CNT composites have been reported. For CNT–epoxy systems, increases in modulus and tensile strength of no more than 30% are typical,[66–69] and more often than not a diminution in strength and elongation at break (related to toughness) are obtained. Bai achieved up to a 200% increase in modulus for a CNT-filled (0.1 to 4 wt-%) epoxy system, but modest improvements in tensile strength with a dramatic reduction in fracture strain.[70,71] The mechanical reinforcement of polymers is controlled by the degree of dispersion and orientation of CNTs in the polymer matrix, the aspect ratio of the CNTs, and the efficiency of stress transfer at the interface between the CNTs and polymer chains.[37] The mechanisms for stress transfer are not well understood, but include chemical bonding, van der Waals-type attractive forces, and mechanical interlocking across the length scales, as proposed by Schadler et al.[28] Specifically with regard to CNT reinforcement of thermosets, other factors such as the effect of CNTs on the crosslink density and cure kinetics,[72] polymer chain mobility[73] (thus glass transition process), and nanotube flexibility[27] are also important factors. In addition, a chemical reaction between reactive thermoset precursors and CNTs can provide a route for the formation of a 3D network for effective stress transfer.[74] Furthermore, there is strong evidence to suggest that CNTs enhance the fracture toughness of polymers, which include epoxies, even for a CNT content of 0.1 wt-%.[47] The CNTs reinforce the matrix by providing a bridging mechanism to resist crack propagation.

The influence of fluorinated and amine-functionalized CNTs on the T_g of different epoxy systems (diglycidyl ether of 9,9-bis(4-hydroxyphenyl) fluorene (DGEBF) and diglycidyl ether of bisphenol A (DGEBA)) was investigated using DMA by Miyagawa and Drzal[73] and Gojny and Schulte,[75] respectively. In the latter study the authors reported an increase in T_g with an increase in CNT loading to 0.8 wt-%, the effect being greater for amine-functionalized CNTs compared with non-functionalized CNTs, and this they concluded was a consequence of the improved interfacial interactions between nanotube and polymer. Conversely, Miyagawa and Drzal obtained significant decreases in T_g, 30°C for a CNT loading of 0.2 wt-%, because of the non-stoichiometry of the epoxy matrix caused by the fluorine groups on the surface of the CNTs.

The fundamental properties of CNT-filled epoxy composites for several other technologies have also been examined, including magnetic susceptibility[76] and thermal conductivity.[77] Many properties of epoxy/CNT composites can be enhanced by alignment of the CNTs during processing. Martin et al.[78] used both AC and DC electric fields to induce the alignment of CNT networks in an epoxy matrix, however, while AC fields yielded more uniform and aligned networks than DC fields, the network efficiency was not improved. Choi et al. demonstrated that magnetic field processing, using fields up to 25 T and temperatures of 60°C, can enhance both the electrical and thermal conductivity of a 3 wt-% CNT-filled epoxy.[79] While it is obvious that the addition of CNTs to epoxy resins alters the cure kinetics of the reaction, and thus the physical properties of the resin, surprisingly few studies on the subject have been published. Puglia et al.,[72] using a combination of thermal analysis and Raman spectroscopy, showed that SWCNTs can act as a strong catalyst for a relatively highly loaded (>5 wt-%) epoxy resin, and the extent of the cure reaction can be greatly altered on the addition of SWCNTs, see Fig. 5.

The incorporation of CNTs into thermosetting polyimides has also been studied by Jiang et al.[80] and Ogasawara et al.[81] A percolation threshold as low as 0.15 vol.-% and an increase of ~11 orders of magnitude in electrical conductivity compared with the neat resin was obtained by Jiang et al. when MWCNTs made by both CVD and a laser ablating technique were added to a

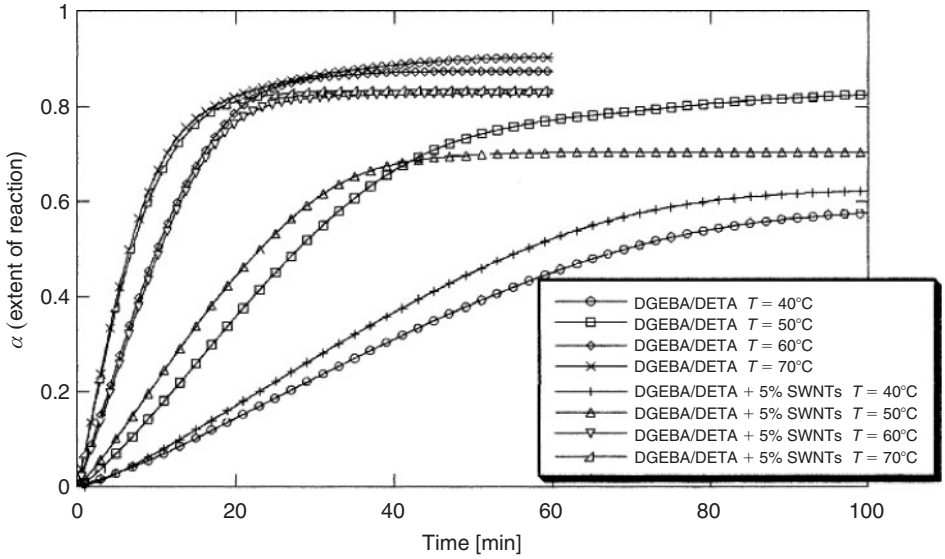

Fig. 5. Extent of reaction (α) versus time at different isothermal temperatures for a DGEBA–DETA system and 5% DGEBA–DETA/SWNT composite. (Reproduced with permission from Wiley Interscience to reproduce from ref. [72].)

polyimide. Ogasawara et al. reported an increase in modulus and strength, but a drop in fracture strain for composites of MWCNTs with a phenylethynyl-terminated polyimide, although loadings as high as 14.3 wt-% were required.

In particular, the electrical properties of CNT-filled epoxies have been investigated. Sandler et al.[19,41] and Martin et al.[42] reported an improved electrical conductivity of ~9 orders of magnitude compared with the neat resin for percolation thresholds well below 0.05 wt-% CNTs. Moreover, Martin et al. also demonstrated a correlation between mean nanotube length and reduced percolation threshold, in that shorter more mobile nanotubes accelerate the rate of network formation to result in a lower percolation threshold, at least for the epoxy system used in their study. Barrau et al. studied the AC and DC conductivities of a CNT-filled bisphenol A-type epoxy resin as a function of temperature.[82] They showed a DC conductivity percolation at 0.3 wt-% and suggest that the main mechanism for conduction is by electron tunnelling. Gojny et al. examined the effect of nanotube type and functionality on electrical conductivity and concluded that any form of functionalization that results in a decrease in aspect ratio of the nanotube results in an increased electrical percolation threshold.[63]

4. Thermoplastic Polymer/CNT Composites

4.1. Solution Mixing and In-Situ Polymerization

The synthesis of polymer/CNT composites in solution is by far the most commonly employed method of processing. Solvent casting, as the name suggests, involves the agitation of CNTs in a solvent or dissolved polymer solution before casting into moulds. The use of a solvent and/or polymer in solution with the introduction of magnetic/mechanical stirring or energetic agitation in the form of ultrasonication to aid dispersion of CNTs is familiar and frequently used in the preparation of new materials. There are obvious limitations of solution processing in that many stages of production are involved and, unlike melt processing, it is not one continuous process. Solution processing is mainly used in the production of CNT/polymer composites where the polymer in question is soluble in common organic solvents or is a thermoset material and melt processing is not a viable option.

A typical example of the solution mixing process is described by Wong et al.[67] MWCNTs synthesized by the pyrolysis of hydrocarbons were initially purified in nitric acid to dissolve the catalyst particles. Polystyrene (PS) was dissolved in toluene by stirring on a hot plate for 30 min. Crucially, the solvent and the agitation process must be capable of dispersing nanotube agglomerations before the evaporation stage. The appropriate mass of nanotubes was added to the warm polymer/toluene solution and stirred for 1 h to form a homogeneous suspension. The mixture was ultrasonicated for a further hour and then cast into aluminium moulds in the form of a film and solvent extraction occurred in an oven at 100°C for 3 h. This example of the solution casting of polymer/MWCNT composites is characteristic of the usual procedures adopted. Variations naturally occur in the choice of suitable solvent for the chosen polymer, agitation method, stirring speeds, and solvent extraction process. In the case of PS, the solution cast method described above was used to form film samples that were then cut into pieces and subsequently melt-mixed in a mini-extruder at 180°C. Extruded rods were then tensile tested with the fractured surfaces examined using FESEM and TEM. Mechanical testing of samples with a nanotube loading from 0.1 to 2.0 wt-%, yielded decreased modulus, tensile strength, and failure strain with respect to the original polymer, with the exception of the 0.1 wt-% sample which showed slight increases (~2–10%) in all three mechanical properties. FESEM images revealed poorly dispersed CNTs, as 5 to 20 μm sized nanotube agglomerations were evident. The reinforcing effect of the nanotubes is surpassed by the nanotube bundles acting as stress-concentration points within the polymer matrix, which reduces the original mechanical properties of the virgin polymer. However, the reinforcing effect of the nanotubes in the 1 wt-% composite can be explained by the slight pull-out and alignment of a nanotube bundle within the agglomerate. Further examination of the FESEM images indicated that the CNTs were all coated with PS. This suggests there is good wetting of the nanotube surface by the polymer because of positive surface energies on contact and TEM imaging revealed 'kinks' and 'twists' in the expected 'smooth' surface of the CNTs. This is thought to contribute to a type of 'mechanical interlocking' in that the rough contacts between the nanotube and polymer

require more energy to separate them than would even surfaces. The authors propose a variety of mechanisms to explain the reinforcement effects of the CNTs although it may seem more worthwhile to return to the root of the problem – the initial dispersion of tubes in the solution cast process. As there seems to be considerable interfacial adhesion between tubes and polymer chains, the problem of dispersion is one that needs to be addressed and improved upon.

The scaling law of percolation theory[83] can be described by Eqn 2 where σ is electrical conductivity, p is the volume fraction of filler, p_c is the critical filler concentration or percolation threshold, and t is the critical exponent:

$$\sigma\alpha(p - p_c)^t. \quad (2)$$

Conductivity exponents of 3D percolating networks have been found in general to have values of $\sim t = 1.65$.[84] The conductivity critical exponent, as a general rule, reflects the dimensionality of the system with values of 1.3 and 2.0 reported for two and three dimensions, respectively.[41] For an epoxy resin/MWCNT composite, Sandler et al. reported values of $p_c = 0.0025$ wt-% and $t = 1.2$ and attributed the low scaling exponent not to a diminution in system dimensionality but the aggregation of MWCNTs during sample preparation.[31] Martin et al. quoted t exponents of 1.78 and 1.74 for epoxy/MWCNT percolated networks of 0.0021 and 0.0039 wt-%, respectively.[42]

The DC conductivity of PMMA/MWCNT samples prepared by solution mixing were reported by Kim et al.[85] and the incorporation of both Fe and Co CVD-produced MWCNTs was investigated. Films were made by the ultrasonication of MWCNTs, poly(methyl methacrylate) (PMMA), and toluene over a period of 24 h and subsequent solvent extraction. The distribution of the nanotubes was described as 'homogeneous' although no evidence of this was provided in the paper. However, the electrical conductivity results, obtained using a four-point probe method, clearly demonstrate that a percolated network of nanotubes had formed throughout the polymer film with a percolation threshold estimated at ~0.003 wt-%. Log–log plots of DC conductivity versus mass fraction of Fe MWCNTs revealed that the conductivity (σ) of PMMA increased by $\sim 10^{10}$ S cm^{-1} on addition of 0.3 wt-% CNTs and the critical exponent of the percolated network was ~2.15.

In other work by Benoit et al. a percolation threshold of 0.33 wt-% was reported for PMMA/SWCNT solution cast composites in tests performed on 10 μm thick samples by the four-point probe method.[86] Du et al. reported that the alignment of SWCNTs in a PMMA composite reduced the electrical conductivity of the 2 wt-% composite from 10^{-4} (unaligned) to 10^{-10} S cm^{-1} (aligned).[87] The electrical conductivity is decreased because of the reduction in the number of electrical contacts due to nanotube orientation. In the studies by Wong et al.[67] and Kim et al.[85] there are similarities in the solution cast process used, yet two inherently different outcomes arise. Kim et al. achieved homogeneous PMMA/MWCNT film samples, which was supported, to a limited extent, by observations from SEM images. An electrically percolated network of MWCNTs was formed, as four-point probe testing on samples revealed a percolation threshold for 0.003 wt-% of MWCNTs. The Fe and Co CVD-produced MWCNTs were used as received, and the polymer, solvent, and nanotube suspension was simply stirred mechanically in an ultrasonic bath for 24 h. Conversely, Wong et al. produced PS/MWCNT samples that contained significant levels of agglomerated material, obvious from SEM imaging. The authors purified the Ni CVD-produced MWCNT

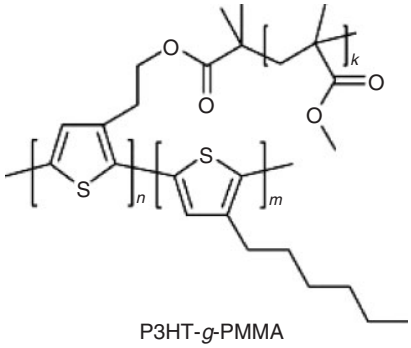

P3HT-*g*-PMMA

Fig. 6. Chemical structure of the compatibilizer, P3HT-*g*-PMMA. (Reproduced with permission from Elsevier to reproduce from ref. [88].)

and used a combination of mechanical stirring (1 h), ultrasonication (1 h), and melt extrusion to disperse the tubes in the PS matrix. Stirring the mixture for an extended period of time in an ultrasonic bath appears to achieve much better mixing results than those using complicated purification and agitation techniques. Tube rupture or fragmentation under the application of sound energy or aggressive acidic boiling reduces the aspect ratio of the tubes and, in turn, reduces the end-performance of the composite material. Polymer choice may have had an affect on the level of dispersion of the nanotubes, as the interactions between PMMA/MWCNTs and PS/MWCNTs will have been different. Several researchers have studied non-covalent functionalization as a means to enhance compatibility between CNTs and PMMA. By way of example, Kim et al. functionalized MWCNTs with poly(3-hexylthiophene)-*graft*-poly(methyl methacrylate) (P3HT-*g*-PMMA) which, when added to the PMMA matrix, were more highly dispersed than unfunctionalized MWCNTs,[88] see Fig. 6. The Young's modulus and tensile strength of the compatibilized systems were greater than those without compatibilizer for the same MWCNT loading.

The thermal conductivity of polymers can also be enhanced by the addition of CNTs. Bonnet et al. obtained a 55% increase in thermal conductivity of PMMA on addition of 7 vol.-% of SWCNTs combined with an increase in electrical conductivity by ~8 orders of magnitude.[89] The authors obtained a thermal conductivity pre-factor in the range 25–55 ± 10 W m^{-1} K^{-1}, values comparable to that reported for unaligned SWCNT buckypaper and ~100 times that of neat PMMA.

Work by Safadi et al. demonstrated that films of PS and MWCNTs, produced by the solvent cast method in toluene using ultrasonic agitation, produced electrically conductive nanocomposites with a percolation threshold value of 0.25 vol.-%.[90] The surface resistivity approached 10^3 Ω cm^{-1} on the addition of 2.5 vol.-% MWCNTs. The level of dispersion required to form an electrically conductive network of untreated tubes was possible by using similar processing steps as in ref. [57] without the use of destructive acid treatment of MWCNTs. In another approach, Byrne et al. functionalized MWCNTs using an organometallic, *n*-butyllithium, to produce MWCNTs that have a butyl functionality,[91] see Fig. 7. The addition of butyl-modified MWCNTs to PS resulted in an increase in both tensile strength and modulus relative to neat PS.

Composites of ultrahigh molecular weight polyethylene (UHMWPE) (6×10^6 g mol^{-1}) and MWCNTs were prepared by solution mixing.[92] Ruan et al. initially purified MWCNTs to remove impurities before dispersing the nanotubes in xylene by magnetic stirring (2 h) and ultrasonication (2 h). The nanotube

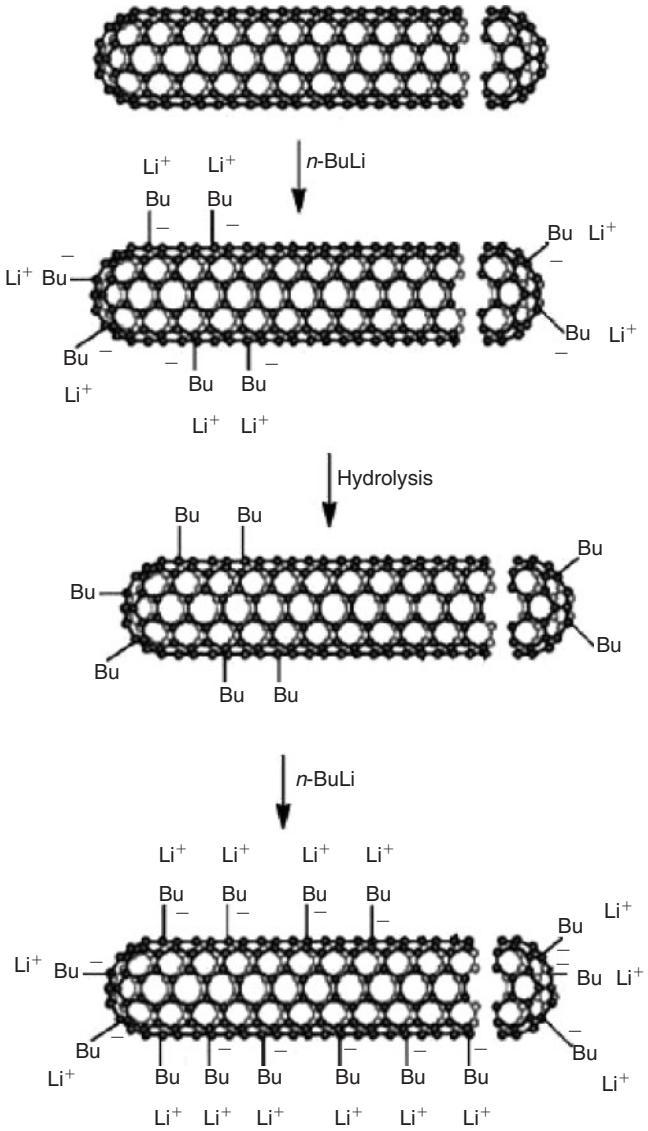

Fig. 7. Reaction scheme for the preparation of butyl-functionalized nanotubes. (Reproduced with permission from IOP to reproduce from ref. [91].)

suspension was then added to a mixture of UHMWPE and xylene and refluxed for 3 h, and composite films were obtained by solution casting followed by tensile drawing. TEM revealed that undrawn film samples contained agglomerations of nanotubes of $\sim$1 μm in diameter and that crystal growth, visible from TEM images, propagated from nucleating sites on the tubes. Viewed at higher magnification, these agglomerations contained loosely agglomerated material. The tensile strength and modulus were improved for the undrawn sample (1 wt-% of CNTs) by 50 and 38%, respectively, and both the tensile strength (25%) and ductility (140%) of the drawn sample that contained MWCNTs improved concomitantly. This improvement in ductility was explained by a process of secondary crystal formation that nucleated from nanotube agglomeration sites. Micro-Raman mechanical spectroscopy indicated good load transfer at the polymer/nanotube interface, which was manifest by shifting of the well-defined Raman bands that corresponded to the crystal form of graphite, the D-band (disorder induced, A_{1g}), the G-band (tangential mode, E_{2g}), and the D* (or G′ band, overtone of the D-band).[92] A shift in a Raman peak position is attributable to changes in the inter-atomic distances within a material as it is deformed, in that the larger the shift, the greater the strain carried by the nanotubes.[24] Acid treatment of the pristine MWCNTs in ref. [92] produced an up-shift of all the Raman peaks as the nanotubes were constricted and packed closer together on removal of particulate impurities. This unambiguously demonstrates the sensitivity and efficiency of Raman spectroscopy in probing the changes to the physical environment of the tubes after chemical treatment or response to applied stresses presented during tensile/compressive deformation or composite formation. Even the incorporation of MWCNTs into a polyethylene (PE) matrix induced a peak shift of several wavenumbers as the formation of PE crystals during solvent extraction exerts a compressive stress on the dispersed tubes.[92] Analysis of the change in peak position of the D* band of the 1 wt-% composite with respect to strain (%) exhibits interesting behaviour in that there are four distinct regions of the spectrum, each representative of characteristic features of how a material behaves under applied tensile loading; elastic response, viscoelastic and plastic deformation, strain hardening, and partial failure. The gradient variations are related to various load transfer and deformation mechanisms. At high strain rates as the polymer material buckles, a large load is transferred to the nanotubes, which results in a sudden increase in shifting of the Raman peak. The focus of the paper by Raun et al.[92] was not only to investigate the load transfer between the UHMWPE and acid-treated MWCNTs under tensile load but also to describe the molecular level deformation behaviour of high-modulus and high-strength UHMWPE fibres using micro-Raman spectroscopy. This spectroscopic method is widely accepted as a model analytical tool for the characterization of SWCNTs, MWCNTs, and their composites.

The use of electrospinning as a method to fabricate polymer/CNT composites is also currently attracting interest. Wang et al. reported the preparation and mechanical properties of electrospun composite fibres of PVA with acid-treated MWCNTs.[93] The tensile strength of the composite materials was greater that non-woven PVA sheets, however, when the MWCNT concentration was above 1 wt-% the tensile strength decreased markedly. Studies on composites of PVA with both SWCNTs and MWCNTs using a range of solutions, including dimethyl sulfoxide (DMSO),[93] deionized water,[94] and water stabilized with either covalent acidic oxidation or by surfactant adsorption[95] have also been reported in the literature. Pan et al. described the use of electrospinning in the part fabrication of hollow fibres of PE and PS/MWCNT composite materials.[96] The nanofibres produced had large surface areas ideal for use in biomedical applications.

In-situ polymerization is ideal for the creation of polymer/CNT composites because of the free radical initiated, addition chain reaction of vinyl monomers at a molecular level. Such intimate mixing is not achievable when a polymer is in the molten or solution state. So in the event of an insoluble or thermally unstable polymer, which cannot be processed by solution or melt processing, in-situ polymerization is often the favoured alternative as it allows the successful preparation of polymer/CNT composites with high nanotube loadings. In addition, polymer molecules can be grafted onto the surface of the CNT during the polymerization process. Direct grafting of polymer to the nanotube surface can promote contact between species at the interface, which results in much improved bulk composite properties. Vinyl polymers such as PMMA and PS are common engineering plastics and are used frequently to form CNT composites by the in-situ polymerization process,[97,98]

although many polymers can be synthesized by this process.[28]

In a study by Yang et al., MMA monomer was initially dried and purified before polymerization.[97] Benzoyl peroxide (BPO) was used as the free radical initiator and polymerization started at 85–90°C and after a period of 1 h CVD-produced CNTs were added and the mixture stirred with the aid of ultrasonication for a further 30 min. The addition of CNTs to the monomer during the polymerization reaction promoted intimate mixing between the polymer and CNTs at a molecular level. The mixture was then transferred to a mould and left to condition for a further 24 h. In further work by the same authors, the same in-situ polymerization process was used to make PS/MWCNT composites,[98] and in both instances the polymer/CNT composites exhibited improved wear resistance in comparison to the virgin polymer. The lubricating properties of MWCNTs are evident in the reduction of wear rate and friction co-efficient of both polymers. Yang et al.[98] concluded, from TEM evidence, the nanotubes were 'uniformly dispersed in the nanocomposites', although the images do not support this conclusion as they are out of focus and appear to show loosely bound agglomerations of catalytically grown MWCNTs.

In earlier work by Jia et al., 2,2′-azoisobutyronitrile (AIBN) was used as the free radical polymerization initiator.[99] It was discovered that AIBN can open the π-bonds in CNTs during the in-situ polymerization process, and this initiation mechanism allows CNTs to bond with PMMA, to form strong interfacial interactions between nanotube and polymer. However, the interference of the CNT species with the polymerization reaction terminates the monomer chain linkage, which yields low-molecular-weight PMMA, with badly dispersed un-treated CNTs and the resulting composite had diminished mechanical properties relative to the original polymer. During further experimentation, the in-situ process was improved by increasing the polymerization time before nanotube addition, which allowed time for the polymer to form while still creating strong polymer–nanotube covalent bonding. In addition, dispersion was aided by separating nanotube agglomerations and reducing nanotube lengths by acidic boiling in concentrated nitric acid. The more controlled reaction of the radical initiator with the π-bonds in the MWCNTs, coupled with better dispersion of acid-treated nanotubes, led to significantly improved mechanical properties of the PMMA/CNT composites. The action of the AIBN initiator, as proposed by Jia et al.,[99] has been corroborated by several other studies on PMMA/CNT[100,101] and PS/CNT[102,103] composites.

Interestingly, the first account of the use of functionalized arc discharge-synthesized CNTs in an in-situ polymerization process was recorded by Velasco-Santos et al.[100] A combination of infrared and Raman spectroscopy was used to confirm the interaction between the functional moieties of the nanotubes and the PMMA groups. Furthermore, IR spectroscopy also suggested that the opening of π-bonds in the untreated CNTs through the action of the AIBN initiator induced polymer–nanotube covalent interactions. The unfunctionalized CNTs increased the T_g of the original polymer by ∼6°C. In contrast, the CNTs with COOH and COO^- groups present increased the T_g of virgin PMMA by a significant 40°C. Improvements were reported in modulus and toughness with a small reduction in elastic behaviour, although increasing the loading of functionalized nanotubes improved the elastic behaviour of the composites. Park et al. used acid-treated, catalytic CVD-produced MWCNTs and AIBN as a radical initiator to synthesize PMMA/CNT composites again by in-situ polymerization.[101] The authors report the evolution of a new Raman peak, evident at 1650 cm^{-1}, that originated from the formation of a C–C bond between the MWCNTs and PMMA during the polymerization process. A four-point probe method was used to assess the electrical properties of the composites and the conductivity increased significantly with the addition of MWCNTs from 10^{-3} S cm^{-1} for electrically insulating neat PMMA, to 3.2×10^{-4}, 2.2×10^{-2}, and 1.7×10^{-1} S cm^{-1} for 1, 5, and 10 wt-% nanotube loadings, respectively.

Wang et al. prepared composites of poly(ethylene terephthalate) (PET) with very low MWCNT contents (from 0.01 to 0.2 wt-%) by in-situ polymerization.[104] The MWCNTs had a significant nucleating effect on PET crystallization, and increased the crystallization temperature of PET by 6°C, but formed smaller crystallites with lower melting temperatures. In another study, Jin et al. also prepared PET/MWCNT composites using in-situ polymerization, however, before composite formation, the surface of the MWCNTs were modified with both carboxylic acid and diamine functional groups,[105] see Fig. 8.

The tensile strength and modulus of these composites increased by 350 and 290%, respectively, in comparison with the composites prepared with pristine MWCNTs. In-situ gamma radiation-induced chemical polymerization at room temperature has also been employed in the preparation of poly(pyrrole) (PPy)/MWCNT composites.[106] A 0.1 M HCl solution of ammonium persulfate was added dropwise to a 0.1 M HCl solution of pyrrole monomer and MWCNTs using sonication, and the resultant solution was de-aerated before being irradiated by a ^{60}C γ-ray source at a rate of 20 kGy for 1 h, under atmospheric pressure and ambient temperature. Characterization of the composites using several techniques revealed that there had been no chemical reaction between the polymer and CNT, rather the MWCNT functions as a template for PPy polymerization. The resulting composites had an electrical conductivity as high as 0.38 S cm^{-1}.

More recently, the potential of atom transfer radical polymerization (ATRP), reversible addition–fragmentation chain transfer polymerization (RAFT), and ring-opening metathesis polymerization (ROMP) has been demonstrated as effective mechanisms for CNT functionalization and composite formation. Polymers grafted onto CNTs will aid the dispersion and dissolution of CNTs in polymer matrices. Covalent attachment of polymer chains to the surfaces of CNTs can normally be achieved using either 'grafting from' or 'grafting to' methodologies. The former is based on the deposition of initiators onto CNTs followed by surface-initiated polymerization, the latter on the reaction between a preformed end-functionalized polymer with reactive groups on the surface of the CNT.[107] Both methods have been used by several authors to modify the surfaces of CNTs, and both covalent and non-covalent attachment of polymers to CNTs has been reviewed by Liu.[108] Qin et al. reported the functionalization of SWCNTs with PS.[109] 'Grafting to' functionalization was successful by cycloaddition of PS-N_3 to the sidewalls of CNTs and grafting from functionalization by ATRP of styrene monomer from SWCNTs pre-functionalized with one ATRP initiator per 240 carbon atoms of the SWCNT. Importantly, the authors reported that the sidewall structure of the SWCNTs was unaltered and the SWCNT bundles were broken up as a consequence of functionalization and polymerization. ATRP has also been used to graft PMMA,[110] PS copolymers,[111–113] and hydroxy-functional poly(glycerol methacrylate)[114] onto CNTs. However, the reports on the use of polymer-functionalized CNTs obtained with ATRP and then

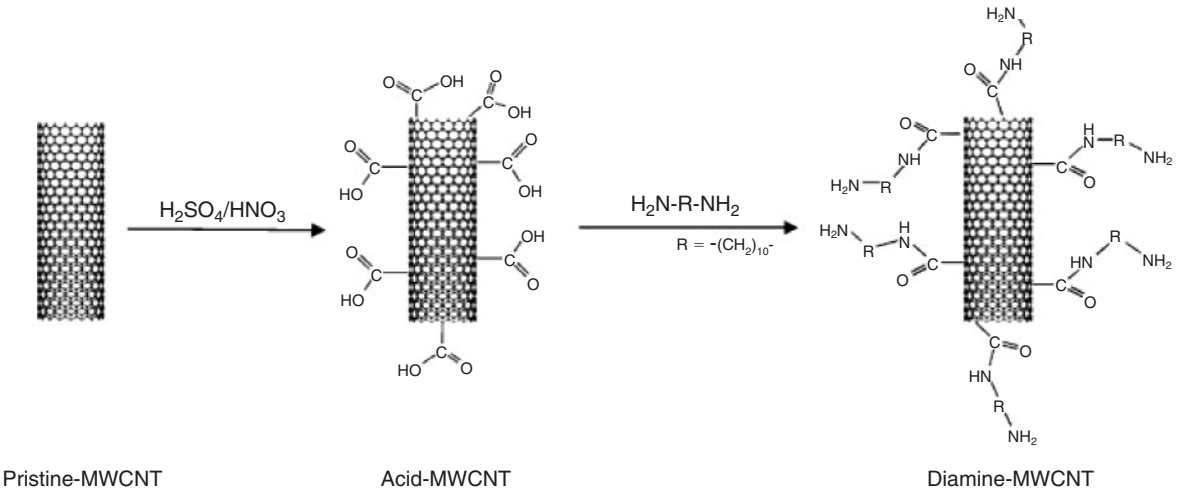

Fig. 8. Schematic representation of the formation of acid-MWCNTs and diamine-MWCNTs. (Reproduced with permission from Elsevier to reproduce from ref. [105].)

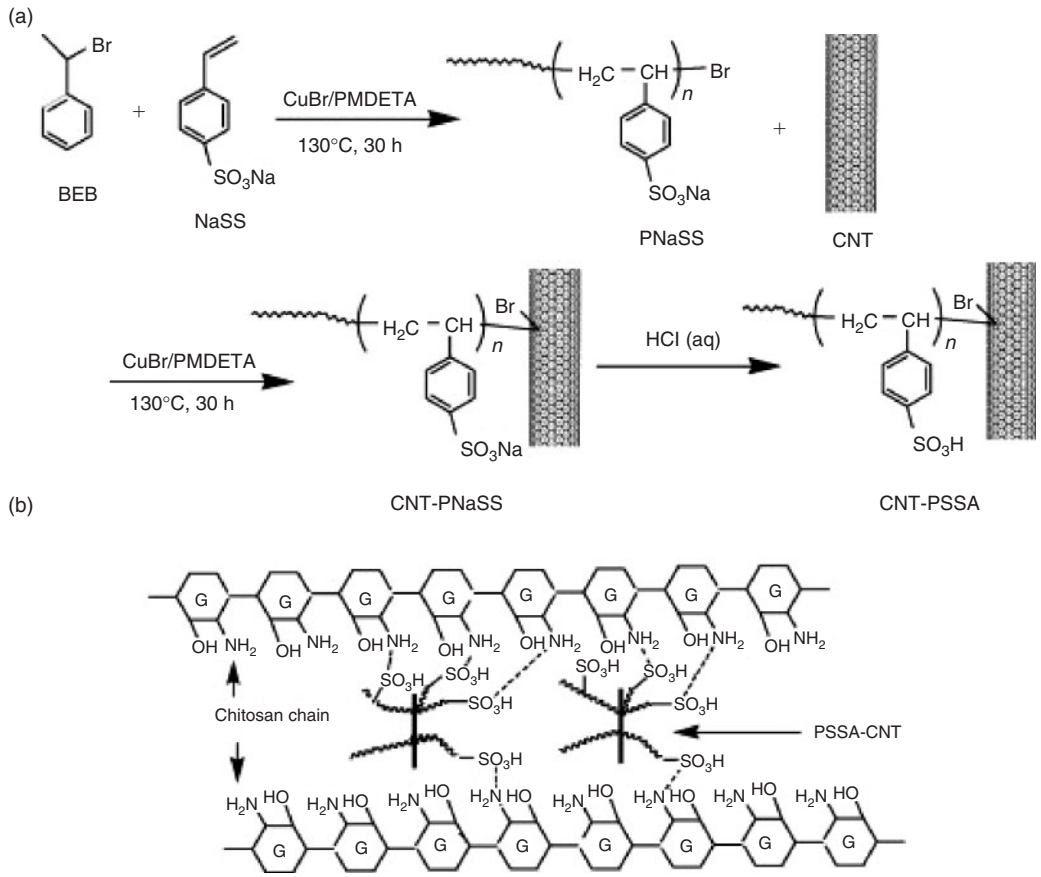

Fig. 9. (a) Preparation of poly(styrene sulfonic acid)-functionalized CNTs (PSSA-CNTs). (b) A model representing the linkages between PSSA-CNTs and chitosan in chitosan/PSSA-CNT nanocomposites. (Reproduced with permission from Elsevier to reproduce from ref. [115].)

utilized in the preparation of polymer/CNT nanocomposites are much less numerous. Liu et al. described the synthesis of poly(styrene sulfonic acid)-functionalized CNTs by ATRP and the preparation of chitosan/CNT nanocomposites using the poly(styrene sulfonic acid)-functionalized CNTs,[115] see Fig. 9.

The sulfonic acid groups enhance the interfacial interaction with chitosan through reaction with the amino groups. The nanocomposites obtained had superior thermal, mechanical, water uptake, and electrical conductivity relative to neat chitosan. Liu et al. also reported the functionalization of MWCNTs with poly(2,6-dimethyl-1,4-phenylene oxide) (PPO), an important engineering plastic, using brominated PPO and ATRP. A layer of PPO of ~4.5 nm coated the CNTs and the resultant nanocomposites had enhanced mechanical and electrical properties compared with neat PPO.[116] Fragneaud et al. studied the effectiveness of PS grafted onto the surface of MWCNTs to alter the interfacial adhesion in PS/CNT composites.[117] The authors proposed that the low molecular

weight of the PS grafted to the surface of the MWCNTs had a plasticising effect which provides lubrication and in turn aids disentanglement of nanotubes. Further studies on the effect of varying the molecular weight of the grafted polymer on polymer/CNT interfacial interactions will be central to achieving efficient stress transfer at the interface in polymer CNT composites.

Polymer chains have also been successfully grafted onto CNTs using RAFT polymerization. Cui et al., in the first instance, attached RAFT agents, prepared by reacting MWCNT-Br and excess PhC(S)SMgBr on the sidewalls of MWCNTs followed by polymerization of styrene.[118] Hong et al. described a method to functionalize MWCNTs using dithioester groups as RAFT agents and subsequent copolymerization of styrene and maleic anhydride.[119] You et al. have reported the direct growth of ionic polymers on the surfaces of MWCNTs using RAFT polymerization.[120] Similarly, several other polymers have been grafted onto mainly MWCNTs,[121–129] but also SWCNTs.[123] Such polymer-coated CNTs prepared using RAFT polymerization could be readily employed as compatibilizers for polymer/CNT nanocomposites.

A further approach for grafting polymers from surfaces has been demonstrated using ROMP.[130,131] Chen et al. reported the attachment of poly(L-lactide) (PLLA) to MWCNTs using surface-initiated ROMP.[132] First, the MWCNTs were functionalized with hydroxy groups and were swollen in either chloroform or DMF and then sonicated on addition of tin(II) 2-ethylhexanoate and L-lactide to form PLLA-grafted MWCNTs. The incorporation of MWCNT-*g*-PPLA to composites of PLLA and MWCNTs improved the tensile modulus of PLLA without a significant reduction in the elongation at break. Jeong and Kessler reported the synthesis of norborene-functionalized MWCNT/poly(dicyclopentadiene) (poly(DCPD)) nanocomposites by ROMP.[133] The authors claimed a 900% enhancement in tensile toughness relative to neat poly(DCPD) for a functionalized MWCNT loading of only 0.4 wt-% combined with modest increases in modulus and strength. The same authors also studied the thermo-mechanical properties of norbornene-functionalized MWCNT reinforced poly(5-ethylidene-2-norborene) (poly(ENB)) synthesized using ROMP.[134] A 300% increase in tensile toughness and a significant increase in elongation was obtained for a 0.8 wt-% addition of norbornene-functionalized MWCNTs. Examination of the fractured surfaces of tensile test specimens using SEM revealed the functionalized MWCNTs to be highly dispersed in the poly(ENB) matrix in contrast to the large agglomerates observed for the composites with unfunctionalized MWCNTs. ROMP has also been used to functionalize SWCNTs. Liu and Andronov oxidatively shortened and functionalized SWCNTs with ruthenium-based olefin metathesis catalysts.[135] These catalysts were shown to be readily effective in the ROMP of norbornene in that high-molecular-weight polymers could be prepared. Moreover, the poly(norbornene)-functionalized SWCNTs were rendered soluble in organic solvents, in direct contrast to the unfunctionalized SWCNTs. On a related theme, Yoon et al. used surface-initiated, ring-opening polymerization of *p*-dioxanone to functionalize shortened SWCNTs.[136] The thermal stability of the composite materials was increased by 20°C compared with neat poly(*p*-dioxanone).

4.2. Melt Processing of Polymer/CNT Composites

Melt processing of thermoplastic polymer/MWCNT composites utilizes conventional polymer processing technologies, thus the process can be adapted to most laboratory and industrial set-ups already in place. Production rates and material outputs are high, although a pre-shearing step can be required to dry-mix the polymer and nanomaterial before compounding, but by and large, the time required for this is minimal. Modern hopper design provides an adequate solution, by offering separate polymer/nanofiller compartments before the melt-mixing process begins. Masterbatch technologies, where the polymer and nanomaterial have already been melt-mixed and pelletized, just simply require polymer dilution and in this instance no previous mixing step is required. The melt-mixing process is simple, clean, does not require the use of environmentally harmful organic solvents and, after the melt-mixing stage, the molten material can be extruded into any shape, tubing, sheet, or pelletized. Pelletized material can also be injection moulded into various bulk test pieces or compression moulded into film samples. The diversity of the range of end products gives it the leading edge over other production processes and provides practical, cost-effective, and very profitable solutions for advanced materials applications. Research into the melt processing of MWCNT/polymer composites is crucial to the understanding of what can be achieved on a large industrial scale with regards to using CNTs as reinforcing fillers in polymers. It is necessary to understand how processing conditions, for example, the shear stresses applied in an extruder or residence times, are correlated with the dispersion of CNTs and thus final material properties. Because of the number of variables involved, fine tuning of the melt-mixing process is required to achieve enhancement of material properties. It is imperative to understand the role the polymer itself, polymer–nanotube and nanotube–nanotube interactions, and the processing methodology employed play in nanocomposite formation. A small number of previous studies describe the melt mixing of PMMA with CNTs. An early study, Jin et al. described how up to 26 wt-% of arc discharge-produced MWCNTs were dispersed in PMMA in a 'Laboratory Mixing Molder' at 200°C.[137] TEM studies revealed the nanotubes to be undamaged by the mixing process and relatively well dispersed with no large agglomerations present. The addition of 26 wt-% of CNTs to PMMA delayed the onset of thermal degradation by 30°C and displayed a 2700% improvement in storage modulus at 120°C. Gorga and Cohen dry blended PMMA with SWCNTs and MWCNTs before extruding the mixtures at 130°C through a cylindrical die and good dispersion was achieved at low nanotube loadings.[138] The successful alignment of nanotubes was observed by melt drawing the extrudate, which resulted in an increase in tensile toughness of 170% with the addition of 1 wt-% of orientated MWCNTs with respect to the original polymer. Haggenmueller et al. used a combination of solvent casting and melt mixing to prepare PMMA/SWCNT films and fibres for electrical and mechanical testing.[139] The cast films prepared were repeatedly broken and compression moulded up to 25 times in order to promote good nanotube dispersion in the final film sample. Optical micrographs revealed that the dispersion improved with each cycle, although nanotube bundles were still evident. The electrical conductivity along the direction of flow during compression moulding was found to increase from 0.118 to 11.5 $S\,m^{-1}$ as the nanotube loading increased from 1.3 to 6.6 wt-%, respectively. However, measurements made normal to the direction of flow gave significantly lower values. The elastic modulus and yield strength of the highly oriented PMMA/SWCNT melt spun fibres increased with nanotube loading and draw ratio.

Functionalization of the nanotube surface has been used as a method to improve the compatibility of MWCNTs with

polymers. Zhou et al. directly modified the surface of MWCNTs with PMMA by emulsion polymerization initiated by AIBN in an aqueous solution of sodium laurel sulfate, and then made a range of composites by further melt mixing with PMMA.[140] The rheological percolation threshold was reduced from 2.5 to 1.5 wt-% by using PMMA-modified MWCNTs. Jin et al. used poly(vinylidene fluoride) (0.5 wt-%) as a coupling agent for MWCNTs and PMMA,[141] which yielded a doubling of the storage modulus at 50°C. Most of the research into PS/MWCNT composites has focussed on in-situ polymerization and solution mixing as the preferred methods of processing.

An increasing number of studies of melt-processed polymer/CNT composites have been reported including PE,[142,143] poly(propylene) (PP),[144] PS,[145] poly(carbonate) (PC),[146] and others[147] as the host polymer. Thostenson et al. used a micrometer-scale twin screw extruder using a screw speed of 100 rpm to impart very high shear forces into molten composites of PS and CVD-grown MWCNTs.[148] The molten mixture was extruded through a rectangular die and this, combined with drawing the extrudate before cooling, achieved highly aligned CNTs embedded in the polymer films. A control was made by compression moulding undrawn samples of the PS and composite samples. Thin slices of composite were ultramicrotomed normal to the flow direction, and TEM imaging revealed a highly oriented nanotube morphology induced by extrusion and melt drawing. The MWCNTs were initially ultrasonicated in a solution of PS and THF to limit the airborne fraction of nanotubes lost and to keep the weight fractions accurate. This pre-processing step basically integrates a solvent cast step into the processing regime, which in a scale-up situation would not be favourable. The authors claimed this step was intended to pre-disperse the tubes on a micrometer-scale, which ensures the least possible mass of nanotubes is lost to the environment. DMA of the drawn and undrawn polymer and nanocomposites was performed at a constant frequency in a controlled force mode. On first glance, dramatic differences are clear from the DMA curves for both sets of samples. The storage modulii at 25°C of the drawn and undrawn nanocomposites increase relative to the drawn and undrawn polymer by 10 and 49%, respectively, and nanotube orientation undoubtedly improved the strength of PS. The loss modulus curve narrowed significantly and the main peak shifted to higher temperatures after nanotube alignment. During the drawing process, the polymer chains are stretched and restricted, which leaves less free volume for chain motion. A higher temperature is, therefore, required to promote chain mobility. Conversely, Du et al. investigated the effect of nanotube alignment on the rheological properties of PMMA/SWCNT composites and reported higher storage modulus values for isotropic samples compared with the aligned SWCNT composites.[149] A similar trend has also been reported for the conductivities of PMMA/SWCNT[101] and PC/MWCNT[26] composites where nanotube alignment induces a loss of electrical conductivity. As the orientation of the nanotubes increases, the conductivity is reduced because of the stretching and separation of the nanotubes beyond the required inter-tube distance for electron transport.

Thostenson et al. also considered the reinforcing mechanism at the nanotube–polymer interface.[148] Close examination of cracks in a CNT composite using TEM showed MWCNTs bridging the cracks while some were broken, but still adhering to the polymer matrix. This is evidence of good surface wetting and the polymer–nanotube adhesion necessary for improved mechanical properties. This mechanical interlocking, first suggested by Schadler et al.,[28] is a viable mechanism for load transfer and explains overall mechanical improvements in the bulk properties of filled PS. Cipriano et al. have described how the electrical conductivity of PS/MWCNT composites, which can be lost during melt processing, can be recovered by melt annealing the composite at temperatures above the T_g of the polymer.[150] The authors proposed that the conductivity is recovered as a consequence of a transition from an aligned CNT morphology, post melt processing and annealing, to facilitate, through viscoelastic relaxation of the polymer, an interconnected CNT network.

A small number of reports on the melt mixing of semicrystalline PE and CNTs have been published. In contrast to the addition of CNTs to amorphous PMMA and PS, MWCNTs have been shown to affect the crystallization kinetics of certain semicrystalline polymer matrices, including PE.[21,151] McNally et al. prepared linear medium density polyethylene (MDPE)/MWCNT composites by melt-compounding using a mini-twin screw extruder.[20] In the final composites the nanotubes exist as agglomerations with some separation of individual tubes. AFM images of extrudate parallel to the direction of flow revealed the nanotubes to be also aligned in this direction and reduced in length. This could be a result of tube rupture under the higher shear forces induced in the mini-extruder, which is required to obtain good dispersion. The authors suggest that the length variation may be a result of the nanotube length protruding normal to the surface under investigation, or perhaps of the ultra-microtoming process. Volume resistivity measurements were performed on the composites and the resistivity of the pure MDPE was reduced from 10^{20} to $10^4\ \Omega\,cm^{-1}$ on addition of 10 wt-% of MWCNTs. The typical sigmoidal-shaped resistivity curve confirmed that a percolation threshold occurred at 7.5 wt-% of MWCNTs. As the temperature of crystallization (T_c) increased by 8°C for the 10 wt-% composites, the MWCNTs were thought to initiate crystal growth during controlled cooling of the composite from the molten state. A similar effect was observed by Wanjale et al. in the preparation of composites of MWCNTs and poly(but-1-ene) (PB).[147] The effect the MWCNTs had on the morphology of the crystal structure of PB was obvious from optical microscopy. The virgin polymer contained very well defined spherulites, but on the addition of MWCNTs a larger number of smaller crystalline structures were formed, which demonstrated that the MWCNTs provided an active surface for the nucleation of the polymer,[147] see Fig. 10.

Conversely, in other studies, this nucleating effect was not obtained upon the addition of MWCNTs to various polyolefin systems.[142,151] In a study by Ferrara et al. the T_c of an LLDPE was not affected by the incorporation of MWCNTs up to 10 wt-% loading.[142] Dondero et al. melt-processed PP/MWCNT composites using twin-screw extrusion.[152] The authors used a melt-drawing apparatus to improve the dispersion and orientation of the nanotubes within the PP matrix, to achieve simultaneous improvements in modulus (138%) and toughness (32%) with the addition of only 0.25 wt-% of MWCNTs. The addition of nanotubes did not affect the overall crystallinity of the composites.

Liang et al. studied the dependence of the electrical properties of LDPE as a function of temperature, dielectric test frequency, and nanotube loading.[143] Composites were melt-processed using a Brabender mixer and subsequently hot-pressed into plates and a series of composites of LDPE/CNT and LDPE/styrene–ethylene/butylene–styrene-*grafted*-maleic anhydride (SEBS-*g*-MA)/CNT were made. For the LDPE/CNT composites a sharp increase in dielectric constant above

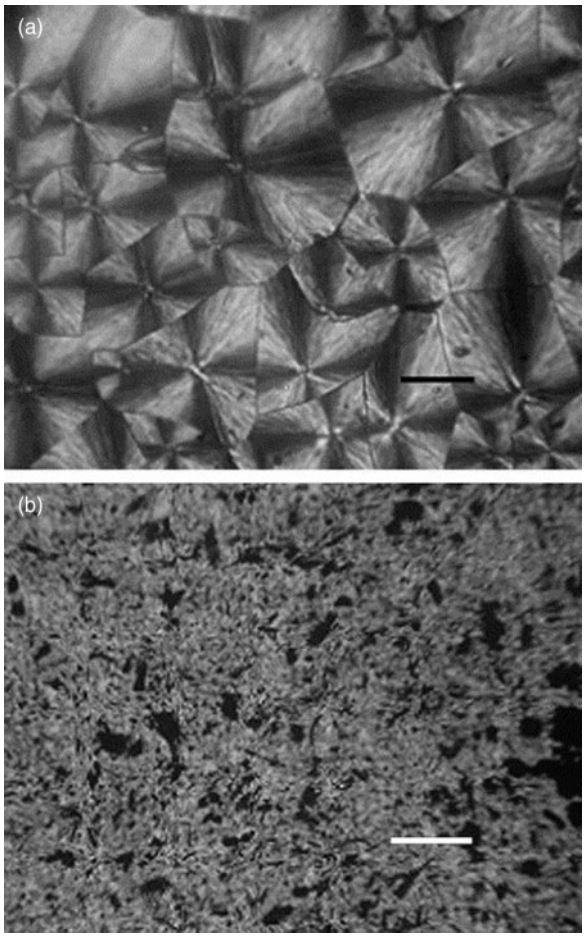

Fig. 10. (a) Optical micrograph of PB (magnification ×100, scale bar 1 cm = 100 μm). (b) Optical micrograph of PB3C (magnification ×100, scale bar 1 cm = 100 μm). (Reproduced with permission from Elsevier to reproduce from ref. [147].)

1.9 vol.-% indicated that an electrically percolating network of nanotubes existed above this nanotube concentration. The composites exhibited typical ohmic behaviour, and the electrical conductivity decreased as the temperature increased. The SEBS-*g*-MA elastomer promoted the dispersion of the CNTs in the LDPE matrix to the extent that an electrically conductive network did not form and the dielectric constant only increased slightly. DMA revealed that the addition of nanotubes increased the T_g of the LDPE by 10°C, which indicates that the addition of the CNTs restricts the molecular motion of the polymer chains. Valentino et al. reported a rheological percolation between 1 and 2.5 wt-% for LDPE and HDPE/MWCNT composites prepared using a micro-twin screw extruder.[144] Large up-shifting in the D and G-bands in the Raman spectra of these composites confirmed that the polymers were exerting a strong compressive force on the MWCNTs.

In another study by Zhang et al., HDPE/SWCNT composites were made by melt-mixing, and a rheological and electrical percolation threshold of ∼1.5 and ∼4 wt-% were recorded, respectively.[153] Optical microscopy revealed SWCNT bundles that were visible to the naked eye above 4 wt-% loading. The electrically conductive network formed is thought to contain pathways of connecting agglomerations and free individual tubes. The addition of 2.6 wt-% High-Pressure CO Conversion (HiPCO) SWCNTs, improved the tensile strength and Young's modulus of the virgin HDPE by 65 and 50%, respectively. The effect of the addition of the nanotubes on the ductility of the polymer was not reported. Manchado et al. produced composites of isotactic PP (iPP) and arc discharge-produced SWCNTs.[145] The modulus of the iPP increased by 40% on the addition of 0.75 wt-% of SWCNTs, and the strength increased from 31 to 36 MPa on the addition of just 0.5 wt-% of SWCNTs. Furthermore, only a slight reduction in elongation at break meant that the nanotubes did not impart a detrimental effect on the toughness of the original iPP. It may be that a good level of nanotube dispersion and distribution in the PP matrix contributed to the improvement of mechanical properties without sacrificing toughness.

The CNT loadings required to achieve a network of conducting particles by melt-mixing is significantly higher than previously recorded for other polymer/MWCNT composites produced by in-situ polymerization and solution processes.[23,45,46] In these papers[23,45,46] using epoxy as the host matrix, the authors report improved electrical conductivity of ∼9 orders of magnitude compared with the neat resin for percolation thresholds occurring well below 0.05 wt-% of CNTs. In particular, Sandler et al., using aligned MWCNTs in an epoxy material, achieved an ultra-low percolation threshold of 0.0025 wt-%.[45] McNally et al. have proposed arguments that may explain why, in general, higher electrical percolation thresholds are observed for the melt-mixing process compared with solution and in-situ polymerization processes.[20] The transfer of electrons required for conduction throughout the bulk sample may be hindered by a layer of polymer (in the order of nanometres thick), which can be observed 'wrapping' the surface of the nanotubes protruding from the composite. A critical minimum distance is required between next nearest neighbour nanotubes to facilitate electron hopping or tunnelling. The layer or film of insulating polymer will provide a tunnelling resistance. Monte Carlo simulations have been used to estimate the maximum tunnelling distance, estimated to be ∼1.8 nm.[154] Alignment of nanotubes from the extrusion process is also considered to be a contributing factor, although conversely, as mentioned above, Sandler et al. used aligned MWCNTs to achieve a very low electrical percolation threshold of 0.0025 wt-% in an epoxy matrix.[41] Linares et al. have also measured the broad-band electrical conductivity of HDPE/MWCNT composites prepared using melt mixing.[155]

More recently, variations in melt processing have been utilized in polymer/CNT composite preparation. Grossiord et al., in the first instance, prepared PS/MWCNT nanocomposites using a latex-based process that consisted of directly mixing an aqueous suspension of MWCNTs in a PS latex stabilized by an anionic surfactant.[156] This mix was then freeze-dried and compression moulded into films at temperatures up to 180°C and processing times that ranged from 2 to 60 min. An electrical percolation threshold of ∼1 wt-% was obtained for these composites. The addition of CNTs to non-commodity polymeric materials, which included biodegradable polymers such as poly(lactic acid) (PLA) for liquid sensing applications,[157] poly(butylene succinate) (PBS) for possible use in electronic packaging materials,[158] and to engineering polymers such as poly(ether ether ketone) (PEEK) for advanced aerospace and electronics components,[159] is gathering interest.

4.3. Raman Spectroscopy of Polymer/CNT Composites

Raman spectroscopy is widely used to investigate both the vibrational and electronic properties of solids,[160] and can be

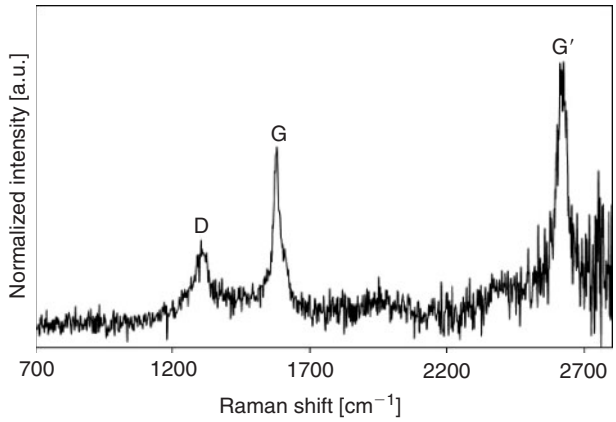

Fig. 11. Raman spectra of CVD-produced MWCNTs in the range 250–3250 cm^{-1}.

performed over a wide range of temperatures and pressures. It is an attractive spectroscopic technique as it offers a quick and simple method of acquiring fundamental information about a material while requiring minimal sample preparation. This non-destructive, analytical tool can be used to identify materials by 'molecular fingerprinting', as specific molecular bonds respond uniquely to Raman laser excitation. The structure of materials can be determined and, although data collection is effortless, the main challenge arises in the interpretation of the Raman spectra.

Raman spectroscopy has been used to identify the diameters of SWCNTs, the diameter distribution of single-walled bundles, and the determination of the chirality and hence the electronic nature of individual nanotubes.[161] An important feature of the Raman spectra of SWCNTs is the radial breathing mode (RBM) (160–300 cm^{-1}) derived from the symmetric movement of carbon atoms in the radial direction.[162] RBM vibrational frequencies are also sensitive to nanotube diameter, and the spectroscopic intensity is also related to the number of tubes present in the sample under investigation. RBMs are difficult to detect for MWCNTs because of the larger diameters involved. Fig. 11 shows several distinctive features of the Raman spectrum of CVD-produced MWCNTs. The MWCNT spectrum is very much like that of graphite and carbon fibres.[163,164]

The D Raman band occurs at 1304 cm^{-1} in the sample analyzed, but generally appears between 1250 and 1450 cm^{-1}. The D or sometimes referred to as the 'disorder'-induced Raman band arises from intrinsic imperfections in the crystalline lattice structure of a nanotube. These defects may be attributed to the imperfect pentagonal or heptagonal arrangements of carbon atoms and the inevitable gaps in the structure that arise as a consequence. Further defect possibilities include the presence of impurities, kinks, and unwanted chemical moieties covalently bonded to the main nanotube structure as by-products of the fabrication process.

The G′ (or D*) band is the second-order overtone of the D-band and occurs at 2626 cm^{-1}. The position of the D and D* bands depends linearly on the incident laser excitation energy.[162] The Raman-active tangential mode or G-band in graphite and MWCNTs is observed at 1582 cm^{-1} and in the region 1500–1700 cm^{-1} for SWCNTs.[162] For the MWCNT sample shown in Fig. 11, the G-band occurs at 1582 cm^{-1}. This peak is derived from the vibrational motion of the carbon atoms, parallel and normal to the axis of the tube itself. The G-band in SWCNTs exhibits a multi-peak feature, where up to six peaks can be observed. The two most intense peaks, labelled G^+ and G^- originate from the break in symmetry caused by rolling a graphene sheet to form a cylindrical shape.[165] It is also possible to identify metallic and semiconducting SWCNTs simply by looking at the features of the tangential Raman mode. Metallic tubes reveal a much broader G^+ peak because of the presence of free electrons, whereas semiconducting tubes have a sharper G^+ peak of much greater intensity than the G^- peak. The Raman frequency, intensity, and band shape of vibrations can vary when nanotubes interact with other species, such as polymers.[162]

Variations in Raman spectra have been observed by simply embedding CNTs in a polymer material. Dieckmann et al. observed changes in the tangential mode of peptide-coated SWCNTs by removing the polymer coating from the nanotubes.[165] Dissolving the polymer and ultra-sonicating the solution subsequently freed the nanotubes from their original positions, which resulted in a change in the G-band and an upshift of >9 cm^{-1} in the RBM. Raman spectroscopy is an invaluable tool when probing the interactions between CNTs and polymers, examining the structure of this interface, and obtaining information about the nature, localization, and force of these interactions.[162] Wood et al. demonstrated the Raman response of SWCNTs embedded in an amorphous unmodified PC matrix as the temperature increased from 100 K to above its T_g (423 K).[166] A correlation was identified between the cohesive energy density (CED) and the Raman response of the D* band. The peak shift of the D* band for the SWCNTs increased from 2625 cm^{-1} above the T_g to ~2645 cm^{-1} at 100 K. As the temperature was reduced, the tubes experienced a compressive force because of thermal stresses exerted by the polymer matrix during shrinkage as the material cools. It is interesting to note here that the position of the D* band remained almost constant on transition through the T_g. The authors clearly demonstrated that only part of the Raman response is a result of thermal effects as further experiments were performed on immersions of SWCNTs in a range of different liquids. The recorded peak shifts were considerably higher for liquids of higher CEDs with the highest shift recorded for water. This work demonstrated the sensitivity of CNTs to molecular forces and shows the potential of CNTs as molecular pressure sensor materials. Lourie et al. demonstrated a similar temperature effect as the D* Raman band of a cured epoxy/nanotube composite shifted to higher frequencies as the mixture was cooled to room temperature.[167]

In work by Puglia et al. Raman spectroscopy was used to highlight how the addition of SWCNTs to an epoxy resin accelerates the cure kinetics and promotes thermal degradation of the resin.[72] The presence of SWCNTs increased the rate of the cure reaction because of the high thermal conductivity of the tubes. The authors argued the separation of the nanotube bundles on addition to the epoxy resin was accountable for the up-shifting of the positions of the RBM and G-band. In turn, the improved intercalation of nanotube bundles increased the thermal degradation of the epoxy resin and accelerated the cure kinetics of the system. The compressive strain the nanotubes experience as a result of the shrinkage of an epoxy resin material can be estimated using Eqn 3, where $\Delta\omega^{\pm}/\omega_0$ is the relative shift of the G band (cm^{-1}), γ is known as the Grüneisen parameter, which describes the frequency shift under hydrostatic strain, approximated to 1.24 for nanotubes,[168] ν_τ is the Poisson ratio of the polymer[169] and taken to be 0.28 in this instance (epoxy), and ε_z is the compressive strain.

$$\Delta\omega^{\pm}/\omega_0 = -\gamma(1 - \nu_\tau)\varepsilon_z. \quad (3)$$

For a 5 wt-% SWCNT loading, $\Delta\omega = 3\,\mathrm{cm}^{-1}$ and ε_z was determined to be -0.21%.[72] This value was eight times less than that reported by McClory et al. using a considerably lower nanotube loading of 0.1 wt-% in a thermoset polyurethane (PU)/MWCNT composite.[74] CNTs are very sensitive and react to changes in their environment and such changes are easily detectable by Raman spectroscopy, which is ideal for the qualitative analysis of CNT–polymer interactions on a molecular scale. Raman spectroscopy can be used to detect load transfer from a polymer matrix to the nanotubes by measuring qualitatively the strain in the nanotubes and, therefore, the load transfer to the nanotubes.[28] Mechanical reinforcement of a polymer matrix by the addition of CNTs involves the transferral of the applied deformation stresses from the polymer matrix to the nanotubes. Efficient transferral of the applied stresses at the polymer–nanotube interface results in overall enhanced mechanical properties with no sacrifice in the strain response of the material. Raman spectroscopy was also used to detect interfacial interactions between a thermoset PU matrix and MWCNTs.[74] The Raman spectra obtained displayed the simultaneous up-shifting and broadening of peaks associated with an isophorone diisocyanate (IPDI) monomer after the addition of only 0.1 wt-% of MWCNTs. This peak shifting is evidence for the interaction of MWCNTs with IPDI by restriction of their natural molecular motion and strong attractive forces between the isocyanate functional group and polar groups at defect sites along the length of the CNTs. Raman spectra of the cured PU composite materials revealed a $24\,\mathrm{cm}^{-1}$ peak up-shift for the G-band, centred at $1582\,\mathrm{cm}^{-1}$. This implies good CNT dispersion and surface wetting of the CNTs by PU, which yielded, relative to the neat PU, simultaneous enhancement in Young's modulus, tensile strength, and ductility by up to 400%, with the addition of only 0.1 wt-% of MWCNTs. Experiments have also been performed to examine how the mechanical deformation behaviour of CNTs can be related to the shifting of the D* Raman band. When a strain is applied to a material, the interatomic distances change, and thus the vibrational frequencies of some of the normal modes change, which causes a Raman peak shift.[169] Schadler et al. reported a $7\,\mathrm{cm}^{-1}$ up-shift in the D* Raman band of an epoxy/MWCNT matrix under a -1% compressive strain using Raman spectroscopy.[28] A more pronounced Raman effect is recorded in compression rather than in tension as only the outer layer of a MWCNT is loaded under tension, as the load is not effectively transferred to the inner layers of the multilayered tube under tension because of the relatively weak bonding between nanotube layers, and also because slippage between concentric nanotubes may occur.[161] Under compression all the layers are loaded, which results in a much larger Raman peak shift as the larger the strain carried by the nanotubes, the larger the Raman peak shift.[28]

Cooper et al. investigated the Raman response of SWCNTs and MWCNTs and their composites under tensile deformation and pressure dependence testing.[170] There was a positive correlation between pressure and the peak shift position of the Raman D* band of the SWCNTs, see Fig. 12. Increasing the compressive stress acting on the SWCNTs by 2 GPa induced an up-shift of $35\,\mathrm{cm}^{-1}$. Under tensile deformation the D* position of the SWCNTs moved to lower frequencies. When comparing the Raman response of different materials under tension and compression it is worth noting the arrangements of nanotubes in space with regards to randomly oriented composites. In a randomly oriented polymer/nanotube composite, some nanotubes will be parallel to and others normal to the direction of the applied tensile or compressive load. This effect, considered by Cooper et al.,[170] is thought to cause a broadening and up-shift of the Raman peak of a randomly oriented CNT composite responding under a compressive force.

4.4. Parallel (Oscillatory) Plate Rheology

Oscillatory melt rheology is a very important analytical tool in the characterization of polymeric materials,[171,172] and has been used extensively to probe the morphology and melt-flow behaviour of a range of filled polymer systems including layered silicates,[173] silica,[174] carbon black,[175] carbon fibres,[176] and CNTs.[177,178] Rheological properties are related to the material's microstructure, the state of nanotube dispersion, the aspect ratio and orientation of nanotubes, and the interactions between nanotubes and polymer chains.[149] A great deal of information can be collated from just one test which can be used to detect the frequency dependence of storage modulus and complex viscosity of composites. At a particular nanotube loading, these values can change notably, which signifies a rheological percolation threshold because of polymer–nanotube interactions. It is well understood that during melt rheology, behaviour at low frequencies is responsive to the changing structure of filled polymer composites. The percolation state of the nanotubes can be detected by a sudden increase in modulus or viscosity as the behaviour of the material becomes less dependent on frequency with increasing filler loading (pseudo-solid-like behaviour).

The level of dispersion of nanotubes in a polymer matrix has a pronounced effect on the rheological properties of CNT nanocomposites. Du et al. reported the effects of nanotube loading, dispersion, alignment, and polymer molecular weight on the rheological behaviour of PMMA/SWCNT composites prepared by a coagulation method.[149] The authors compared the rheological and electrical properties of the composites in an attempt to understand the relationship between the microstructure and rheological properties of the nanocomposites. Nanotube loadings as low as 0.2 wt-% had a significant effect on the viscoelastic properties of the PMMA studied, particularly at low frequencies where the rheometer is more sensitive to changes in storage modulus (G') and loss modulus (G''). At 200°C and low frequencies, the PMMA polymer chains are able to relax and respond to sudden changes in the rate of oscillation. However, the addition of nanotubes to the polymer constricts the relaxed nature of the polymer chains as the presence of nanotubes restrains this motion and hinders the relaxation of polymer chains. Correspondingly, G' and G'' become almost independent of frequency, which indicates the polymer is experiencing 'liquid' to 'solid-like' viscoelastic behaviour, see Fig. 13.

A power law relationship can also be used to determine rheological percolation (analogous to Eqn 2) of the composites (Eqn 4):

$$G'\alpha(m - m_{cG'})^{\beta_{G'}}, \tag{4}$$

where G' is the storage modulus, m is the nanotube mass fraction, $m_{cG'}$ is the rheological percolation threshold, and $\beta_{G'}$ is a critical exponent. Du et al. used Eqns 4 and 2 to determine a rheological percolation threshold of 0.12 wt-% ($0.5\,\mathrm{rad\,s}^{-1}$) and an electrical percolation threshold of 0.39 wt-%, respectively. The critical exponent values determined for the rheological and electrical nanotube networks formed were 0.7 and 2.3, respectively. The larger critical exponent for the electrical network of nanotubes describes the 3D nature of the network required to permit electron conduction throughout the entire sample. The lower critical exponent of 0.7 reported for the rheological situation is

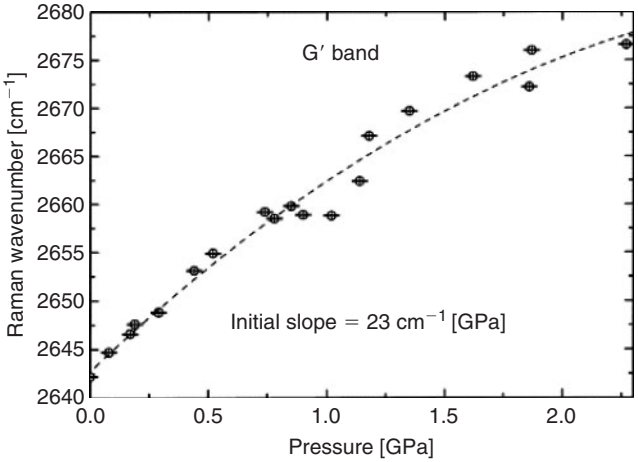

Fig. 12. Pressure dependence of the SWCNT-*P* (2639 cm^{-1}) G′ Raman peak. (Reproduced with permission from Elsevier to reproduce from ref. [170].)

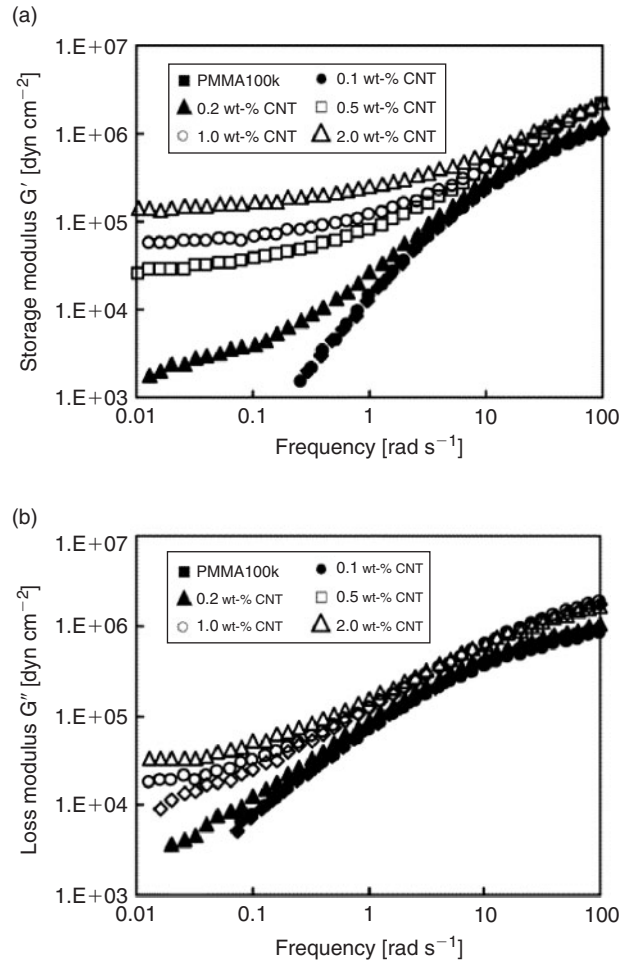

Fig. 13. (a) Storage modulus and (b) loss modulus of SWNT/PMMA nanocomposites with various nanotube loadings. Rheology performed at 200°C and 0.5% strain. (Reproduced with permission from American Chemical Society to reproduce from ref. [149].)

in agreement with a system dimensionality of two. Similarly, Hu et al. also used the power law relationships in Eqns 2 and 4 to determine the electrical and rheological percolation thresholds and the network dimensionality of PET/MWCNT composites prepared by a coagulation method.[178] A rheological percolation threshold of 0.6 wt-% ($t = 1.5$) and an electrical percolation threshold of 0.9 wt-% ($t = 2.2$) were determined. These values are comparable to those reported for PMMA/MWCNT composites by other researchers.[87,149] Kota et al. determined the rheological percolation of PS/MWCNT nanocomposites using dynamic rheological measurements.[179] The authors demonstrated that by quantitatively comparing the normalized log values of electrical conductivity and rheological parameters for a given CNT concentration range, G', G'/G'', and σ_c (electrical conductivity) were more sensitive to percolation compared with η^* (complex viscosity) and G'. Interestingly, both rheological and electrical percolations exhibited sensitivity to the solvent used to prepare the PS/MWCNT composite film.

The variation in rheological and electrical percolation thresholds can be explained by the requirement of a higher CNT loading to reach an electrical percolation threshold than a rheological percolation threshold. Closer nanotube contacts are necessary to conduct electricity by electron hopping (~2 nm) than is required to restrict polymer chain motion in the case of a rheological percolation threshold. Furthermore, not every nanotube contributes to the conduction of electrons, whereas all nanotubes contribute to the restriction of polymer motion. Conversely, McNally et al. reported the electrical and rheological percolation of melt-processed linear MDPE/MWCNT composites to both occur at the same loading of CNTs, 7.5 wt-%, but suggest that this may be purely coincidental.[20]

5. Potential Applications of Polymer/CNT Composites

Numerous potential applications for polymer/CNT composites have been proposed across a broad range of industries, including aerospace, automotive, biomedical, and electronic. As was the case for polymer/nanoclay-based composites, the widespread commercial exploitation of polymer/CNT composites has yet to be fully realized. While it is understood that CNTs are and will be used in a similar way to conventional polymer fillers for mechanical reinforcement and electrical conductivity, here, we highlight some of the more novel, high technology potential applications of polymer/CNT composites.

Most recently, the use of polymer/CNT composites as vapour/liquid and infrared sensors has been proposed. Castro et al. described the role of CNTs grafted with poly(ε-caprolactone) (PCL) in vapour sensing.[180] Grafting of ε-caprolactone from MWCNTs was achieved by in-situ ring-opening polymerization, and conductive polymer composite (CPC) transducers were fabricated by the layer-by-layer spraying of PCL–MWCNT solutions. The authors recorded the chemo-electrical response of these sensors to a range of vapours, including water, methanol, toluene, THF, and chloroform, and demonstrated that such composites could be used quantitatively for detection. Most interestingly, they were sensitive to both polar and non-polar analytes and the PCL-grafted MWCNTs provided an increased sensor response amplitude. In an alternative approach, Kobashi et al. reported the liquid sensing properties of poly(lactic acid)/MWCNT composites prepared using melt mixing in a twin-screw extruder.[181] The electrical resistance of thin films of the composites was monitored during immersion and drying cycles after contact with various solvents, including toluene, chloroform, THF, and ethanol, as a function of time. The changes in resistance obtained were significantly affected by MWCNT loading, and the solubility parameter could be used as an indicator of sensor sensitivity.

Pumera et al. compared the electrochemical sensing properties of a CNT/epoxy composite with that of a graphite/epoxy composite using cyclic voltammetry.[182] The electrodes fabricated with a CNT/epoxy composite (CNT $l = 200\,\mu m$) showed enhanced sensitivity for ferricyanide, nicotinamide adenine dinucleotide (NADH), and hydrogen peroxide, while a composite that contained much shorter tubes ($l = 2\,\mu m$) displayed oxidation potentials for NADH and hydrogen peroxide similar to that obtained for graphite–epoxy electrodes. This suggests that CNT/epoxy composites could be used for bio-sensing applications. The use of polymer/CNT composites as infrared sensors has been demonstrated by Pradhan et al.[183] The authors used poly(phenylene ethynylene)s to non-covalently functionalize and solubilize SWCNTs before dispersion in PC. A SWCNT/PC composite solution was cast onto a glass substrate and dried slowly to produce free-standing films. The composite films obtained were mechanically robust, excellent electrical conductors, and easily fabricated into IR sensor devices. SWCNT type and CNT–polymer–CNT junctions have a significant effect on the electro-optical properties of polymer/SWCNT composites. Moreover, the results presented clearly demonstrated that such composites have potential applications as un-cooled infrared sensors and remotely controlled actuators.

Much attention has been given to the actuation properties of polymer/CNT composites, with particular focus on a possible application as replacement for skeletal muscle, since the phenomenon was first reported for SWCNTs by Baughman et al. in 1999.[184] Conceptually, the combined high Young's modulus and electrically conductivity of CNTs make them an obvious candidate for incorporation into intrinsically conducting polymers, such as PPy and polyanaline (PAn), for actuator materials. Spinks et al. measured the actuation behaviour of layered composites of PAn/CNT/PPy.[185] While the PAn/CNT/PPy composites had lower actuation strains relative to composites without CNTs, the actuation under load was improved on addition of CNTs. Stresses in excess of 10 MPa could be applied to PAn/CNT/PPy composites, but composites without CNTs added failed mechanically at low stresses. Lee et al. studied the electro-mechanical actuation performance of MWCNT/Nafion composites as a function of MWCNT loading.[186] The optimum actuation performance was obtained when the MWCNT loading was 1 wt-%. Above 1 wt-% the MWCNTs were bundled and not uniformly dispersed in the Nafion matrix and resulted in poor electro-mechanical performance.

CNTs will most certainly have an impact in tissue engineering, most notably as reinforcement for tissue scaffolds.[187] For tissue engineering applications, MWCNTs have been incorporated into a range of matrix materials, including chitosan and collagen. In addition to structural reinforcement, CNTs and polymer/CNT composites can be functionalized to provide a mechanism for release of bioactive molecules and support the growth of cells. Shi et al. reported the fabrication of poly(propylene fumarate) (PPF)/SWCNT composite scaffolds for bone tissue engineering.[188] Both unfunctionalized and dodecylated SWCNTs were utilized and the authors investigated the effect of CNTs on pore structure and mechanical properties of PPF scaffolds. It is noteworthy to point out that ultra-short SWCNTs ($l = 20$–$80\,nm$) were used in this study, which had been produced by fluorination and pyrolysis. The dodecylated SWCNT PPF nanocomposites had higher compressive modulus, offset yield strength, and compressive strength compared with neat PPF and the composites with unfunctionalized SWCNTs. In a related paper, Sitharaman et al. investigated the in-vivo biocompatibility of the composites described in ref. [188].[189] The in-vivo biocompatibility of the CNT-filled PPF was similar to neat PPF and the tissue response was comparable to other polymers and polymer nanocomposites.

Other biomedical applications of polymer/CNT composites include in drug delivery and as dental and orthopaedic materials. Kumar et al. reported the functionalization of MWCNTs with poly(2-hydroxyethyl methacrylate) (poly(HEMA)), a hydrogel with excellent biocompatibility and used extensively in drug, dental, and ophthalmic applications.[190] MWCNTs were grafted with HEMA monomer and polymerized by a free radical mechanism using AIBN. Composites of poly(HEMA) with functionalized CNTs were soluble in methanol in contrast to composites prepared with unfunctionalized CNTs. 'Composite' structures of aligned dense arrays of MWCNTs impregnated with polymers have been proposed as nanoporous membranes having high porosity, which are ideal for active drug delivery. Majumder et al., in an attempt to mimic natural protein channels, spin cast PS over the surface of aligned MWCNT arrays and used a H_2O plasma enhanced oxidation process to remove excess PS on the surface of the array and end-cap the MWCNTs.[191] The authors propose that gas flow through such membranes can be enhanced by 1 to 2 orders of magnitude and fluid flow by 4 to 5 orders of magnitude relative to conventional drug membrane materials. Sugars and other biologically active molecules can also be incorporated into CNT composites. Lee et al. prepared glycopolymer/MWCNT composites by grafting the polymer by surface initiated ATRP, the 'grafting from' technique.[192] The approach described by the authors could be employed to copolymerize polysaccharides onto the surface of CNTs, to form hybrid structures which could be used in pathogen detection and as biosensors. Zhou and coworkers, for a very novel application of polymer/CNT composites, developed an interpenetrating polymer network (IPN) of linear poly(acrylamide) (PA) and poly(*N*,*N*-dimethylacrylamide) (PDMA) with PDMA-functionalized MWCNTs, the latter was prepared by ATRP.[193] The double-network composite formed was evaluated as a sieving matrix for DNA sequencing by capillary electrophoresis. The separation provided when MWCNTs were added to the IPN network, combined with higher resolution, and increased speed and reproducibility, make such composite networks ideal for DNA sequencing. A novel tubular morphology was obtained which consists of a rigid PDMA–MWCNT network and a flexible PA–PDMA IPN network. Irrespective of the biomedical or bioengineering applications of polymer/CNT composites, the toxicology and pharmacology of CNTs and polymer/CNT composites needs to be investigated in detail. Results of toxicology studies published to date have been limited,[194] and in many instances contradictory. Fortuitously, surface functionalization can render CNTs water soluble and as such compatible with bodily fluids to provide a path for renal excretion.

Further exciting developments of polymer/CNT composites combine the mechanical and electrical properties of CNTs with shape memory polymers for application as electromagnetic interference shielding (EMI) materials. Zhang et al. reported the EMI behaviour of a CNT-filled shape memory PU as a function of CNT loading and sample thickness.[195] There was a strong correlation between EMI shielding effect and CNT loading and sample thickness, irrespective of frequency. Sahoo et al. investigated the thermal, mechanical, and electro-active shape memory properties of MWCNT and PPy-coated MWCNT filled shape memory polyurethane.[196] As expected, the highest conductivity was achieved for the composites with PPy-coated MWCNTs

(0.098 S cm^{-1}). This conductivity was sufficient such that these composites exhibited an electro-active shape recovery when heated above the PU T_g (40–48°C). The authors claimed a shape recovery between 90 and 95% for an applied voltage of 25 V.

6. Concluding Remarks

While there is no doubt that composite technology is the first large-scale commercially exploitable application of CNTs, there remains several challenges before the extraordinary properties of CNTs can be fully translated to polymeric materials. These include:

1. The purity and defect density of CNTs: Ideally, manufacturers of CNTs should be able to produce very high purity CNTs (>99.9%) without the need for secondary purification, as many methods used involve washing in acid/base which can destroy the tubes. Many of the impurities currently produced, which include amorphous carbon and the oxides of the catalyst metals used, can degrade polymers and alter the electrical properties of CNTs. High levels of defects along the nanotubes will also effect the fundamental ballistic conductance of CNTs.
2. CNT aspect ratio: As is the case with conventional filler technology, the filler aspect ratio has a significant effect on the bulk mechanical properties of a composite material. Further systematic studies need to be completed where composites of polymers with CNTs that have a broad range of aspect ratios are prepared and the dispersion states correlated with composite properties, including but not limited to mechanical, electrical, and rheological properties.
3. Surface functionalization: Several studies have demonstrated that covalent functionalization of CNTs with carboxylic acid, amine, or fluorine groups aids dispersion of CNTs in polymers and subsequently enhances the mechanical and in some instances thermal properties of the matrix polymer. However, covalent functionalization can destroy the intrinsic electrical properties of CNTs. Non-covalent functionalization, through π–π stacking or the use of compatibilizers, has also been used to improve the degree of dispersion of CNTs in polymers. Both methods can promote strong interfacial interactions between CNTs and polymer and contribute to efficient stress transfer at the interface between the CNT and polymer chains. However, difficulties arise when there is a requirement for combined enhancement in electrical conductivity and mechanical properties. An alternative approach is to incorporate other fillers in combination with CNTs to acquire the functionality desired. Many of the 'wet chemistry' methodologies used to functionalize CNTs can also result in tube scission and end-capping. The use of 'dry' methods to functionalize CNTs, such as with plasmas, is currently under investigation.
4. Dispersion of CNTs in polymer matrices: As is the case with most fillers, whether micro- or nanofillers, there remains the challenge of efficiently dispersing and distributing CNTs in polymer matrices. Large-scale use of polymer/CNT composites will only be realized if CNTs can be readily dispersed in molten polymers using conventional polymer processing equipment, such as extrusion and injection moulding, although fibre spinning from both the melt and solution are increasingly of interest. Studies are underway in various laboratories to investigate ways to aid dispersion of CNTs in polymer melts during mixing using ultrasonication, electrical and magnetic fields, and supercritical fluids.
5. Characterization of polymer/CNT composites: Many properties of polymer/CNT composites are governed by the degree of dispersion and distribution of CNTs in the matrix material. Hitherto, many authors have relied too heavily on microscopic evidence in isolation to elucidate the dispersion state, which at worst is misleading and at best only representative. A combined approach that includes the use of techniques such as electrical resistivity measurements, dielectric spectroscopy, impedance spectroscopy, oscillatory rheology, and X-ray tomography with electron microscopy would provide more detail on the dispersion state and the formation of percolated networks. Fundamentally, the interface between polymer chains and CNTs needs to be characterized in detail so that the mechanism(s) of stress transfer in these composites can be understood. Only then will the extraordinary strength of the CNTs be translated to polymeric materials.

While much work stills needs to be done, polymer/CNT composites offer immense potential with application in many fields, including but not limited to, aerospace, automotive, electronic, technical textiles, bioengineering, military, and medical device technologies. However, the challenges listed above must first be met.

Acknowledgements

The authors acknowledge the support of the EU through Specific Targeted Research Project DESYGN-IT (No. NMP4-CT-2004-505626) and S.J.C. is grateful to QUB for funding a studentship.

References

[1] P. M. Ajayan, O. Stephan, C. Colliex, D. Trauth, *Science* **1994**, *265*, 1212. doi:10.1126/SCIENCE.265.5176.1212
[2] http://apps.isiknowledge.com, accessed February 2009.
[3] L. V. Radushkevish, V. M. Lukyanovich, *Zurn. Fisic. Chim.* **1952**, *28*, 88.
[4] A. Oberlin, M. Endo, T. Koyama, *J. Cryst. Growth* **1976**, *32*, 335. doi:10.1016/0022-0248(76)90115-9
[5] T. Edison, *U.S. Patent 223 898* **1880**.
[6] C. Li, E. T. Thostenson, T.-W. Chou, *Compos. Sci. Technol.* **2008**, *68*, 1227. doi:10.1016/J.COMPSCITECH.2008.01.006
[7] S. V. Ahir, Y. Y. Huang, E. M. Terentjev, *Polymer* **2008**, *49*, 3841. doi:10.1016/J.POLYMER.2008.05.005
[8] L. Bokobza, *Polymer* **2007**, *48*, 4907. doi:10.1016/J.POLYMER.2007.06.046
[9] J.-H. Du, J. Bai, H.-M. Cheng, *eXPRESS Polym. Lett.* **2007**, *1*, 253. doi:10.3144/EXPRESSPOLYMLETT.2007.39
[10] M. Moniruzzaman, K. Winey, *Macromolecules* **2006**, *39*, 5194. doi:10.1021/MA060733P
[11] J. N. Coleman, U. Khan, W. J. Blau, Y. K. Gun'ko, *Carbon* **2006**, *44*, 1624. doi:10.1016/J.CARBON.2006.02.038
[12] A. V. Desai, M. A. Haque, *Thin-walled Struct.* **2005**, *43*, 1787. doi:10.1016/J.TWS.2005.07.003
[13] R. Andrews, M. C. Weisenberger, *Curr. Opin. Solid State Mater. Sci.* **2004**, *8*, 31. doi:10.1016/J.COSSMS.2003.10.006
[14] O. Breuer, U. Sundararaj, *Polym. Compos.* **2004**, *25*, 630. doi:10.1002/PC.20058
[15] K.-T. Lau, D. Hui, *Compos. Part B: Eng.* **2002**, *33*, 263. doi:10.1016/S1359-8368(02)00012-4
[16] E. T. Thostenson, Z. Ren, T.-W. Chou, *Compos. Sci. Technol.* **2001**, *61*, 1899. doi:10.1016/S0266-3538(01)00094-X
[17] Q. H. Wang, A. A. Setlur, J. M. Lauerhaas, J. Y. Dai, E. W. Seelig, R. P. H. Chang, *Appl. Phys. Lett.* **1998**, *72*, 2912. doi:10.1063/1.121493
[18] S. A. Curran, P. M. Ajayan, W. J. Blau, D. L. Carroll, J. N. Coleman, A. B. Dalton, A. P. Davey, A. Drury, B. McCarthy, S. Maier, A. Strevens, *Adv. Mater.* **1998**, *10*, 1091.

doi:10.1002/(SICI)1521-4095(199810)10:14<1091::AID-ADMA1091>3.0.CO;2-L

[19] J. Sandler, M. S. P. Shaffer, T. Prasse, W. Bauhofer, K. Schulte, A. H. Windle, *Polymer* **1999**, *40*, 5967. doi:10.1016/S0032-3861(99)00166-4

[20] T. McNally, P. Pötschke, P. Halley, M. Murphy, D. Martin, S. E. J. Bell, G. P. Brennan, D. Bien, P. Lemoine, J. P. Quinn, *Polymer* **2005**, *46*, 8222. doi:10.1016/J.POLYMER.2005.06.094

[21] A. Bhattacharyya, T. Sreekumar, T. Liu, S. Kumar, L. Ericson, R. Hauge, R. Smalley, *Polymer* **2003**, *44*, 2373. doi:10.1016/S0032-3861(03)00073-9

[22] M. Treacy, T. Ebbesen, J. Gibson, *Nature* **1996**, *381*, 678. doi:10.1038/381678A0

[23] R. D. Ruoff, J. Tersoff, D. C. Lorents, S. Subramoney, B. Chan, *Nature* **1993**, *364*, 514. doi:10.1038/364514A0

[24] H. D. Wagner, O. Lourie, Y. Feldman, R. Tenne, *Appl. Phys. Lett.* **1998**, *72*, 188. doi:10.1063/1.120680

[25] A. Kelly, W. R. Tyson, *J. Mech. Phys. Solids* **1965**, *13*, 329. doi:10.1016/0022-5096(65)90035-9

[26] P. Pötschke, H. Brunig, A. Janke, D. Fischer, D. Jehnichen, *Polymer* **2005**, *46*, 10355. doi:10.1016/J.POLYMER.2005.07.106

[27] O. Lourie, D. M. Cox, H. D. Wagner, *Phys. Rev. Lett.* **1998**, *81*, 1638. doi:10.1103/PHYSREVLETT.81.1638

[28] L. S. Schadler, S. C. Giannaris, P. M. Ajayan, *Appl. Phys. Lett.* **1998**, *73*, 3842. doi:10.1063/1.122911

[29] M. S. P. Shaffer, A. H. Windle, *Adv. Mater.* **1999**, *11*, 937. doi:10.1002/(SICI)1521-4095(199908)11:11<937::AID-ADMA937>3.0.CO;2-9

[30] T. Kashiwagi, F. Du, K. I. Winey, K. Groth, J. Shields, *Polymer* **2005**, *46*, 471. doi:10.1016/J.POLYMER.2004.10.087

[31] D. Zilli, C. Chiliotte, M. Escobar, V. Bekeris, G. Rubiolo, A. Cukierman, S. Goyanes, *Polymer* **2005**, *46*, 6090. doi:10.1016/J.POLYMER.2005.04.086

[32] Á. Kukovecz, T. Kanyó, Z. Kónya, I. Kiricsi, *Carbon* **2005**, *43*, 994. doi:10.1016/J.CARBON.2004.11.030

[33] X. Gong, J. Liu, S. Baskaran, R. Voise, J. Young, *J. Chem. Mater.* **2000**, *12*, 1049. doi:10.1021/CM9906396

[34] S. L. Ruan, P. Gao, X. G. Yang, T. X. Yu, *Polymer* **2003**, *44*, 5643. doi:10.1016/S0032-3861(03)00628-1

[35] X. Jiang, Y. Bin, M. Matsuo, *Polymer* **2005**, *46*, 7418. doi:10.1016/J.POLYMER.2005.05.127

[36] J. Sung, H. S. Kim, H. Jin, H. J. Choi, I. Chin, *Macromolecules* **2004**, *37*, 9899. doi:10.1021/MA048355G

[37] B. Khare, P. Wilhite, M. Meyyappan, *Nanotechnology* **2004**, *15*, 1650. doi:10.1088/0957-4484/15/11/048

[38] R. F. Gibson, E. O. Ayorinde, Y.-F. Wen, *Compos. Sci. Technol.* **2007**, *67*, 1. doi:10.1016/J.COMPSCITECH.2006.03.031

[39] O. Lourie, H. D. Wagner, *Compos. Sci. Technol.* **1999**, *59*, 975. doi:10.1016/S0266-3538(98)00148-1

[40] Q. Zhao, M. Frogely, H. D. Wagner, *Polym. Adv. Technol.* **2002**, *13*, 759. doi:10.1002/PAT.246

[41] J. K. W. Sandler, J. E. Kirk, I. A. Kinloch, M. S. P. Shaffer, A. H. Windle, *Polymer* **2003**, *44*, 5893. doi:10.1016/S0032-3861(03)00539-1

[42] C. A. Martin, J. K. W. Sandler, M. S. P. Shaffer, M.-K. Schwarz, W. Bauhofer, K. Schulte, A. H. Windle, *Compos. Sci. Technol.* **2004**, *64*, 2309. doi:10.1016/J.COMPSCITECH.2004.01.025

[43] J. Zhu, J. Kim, H. Peng, J. L. Margrave, V. N. Khabashesku, E. V. Barrera, *Nano Lett.* **2003**, *3*, 1107. doi:10.1021/NL0342489

[44] V. G. Hadjiev, D. C. Lagoudas, E.-S. Oh, P. Thakre, D. Davis, B. S. Files, L. Yowell, S. Arepalli, J. L. Bahr, J. M. Tour, *Compos. Sci. Technol.* **2006**, *66*, 128. doi:10.1016/J.COMPSCITECH.2005.01.004

[45] R. Schüeler, J. Petermann, K. Schulte, H.-P. Wentzel, *J. Appl. Polym. Sci.* **1997**, *63*, 1741. doi:10.1002/(SICI)1097-4628(19970328)63:13<1741::AID-APP5>3.0.CO;2-G

[46] R. J. Hunter, in *Foundations of Colloid Science* **1987**, Vol. 1 (Clarendon Press: Oxford).

[47] T. Prasse, L. Flandin, K. Schulte, W. Bauhofer, *Appl. Phys. Lett.* **1998**, *72*, 2903. doi:10.1063/1.121454

[48] H. Chen, O. Jacobs, W. Wu, G. Rüdiger, B. Schädel, *Polym. Test.* **2007**, *26*, 351. doi:10.1016/J.POLYMERTESTING.2006.11.004

[49] K. L. Lu, R. M. Lago, Y. K. Chen, M. L. H. Green, P. J. F. Harris, S. C. Tsang, *Carbon* **1996**, *34*, 814. doi:10.1016/0008-6223(96)89470-X

[50] K. B. Shelimov, R. O. Esenaliev, A. G. Rinzler, C. B. Huffman, R. E. Smalley, *Chem. Phys. Lett.* **1998**, *282*, 429. doi:10.1016/S0009-2614(97)01265-7

[51] K.-T. Lau, M. Lu, L. Chun-ki, H.-Y. Cheung, F.-L. Sheng, H.-L. Li, *Compos. Sci. Technol.* **2005**, *65*, 719. doi:10.1016/J.COMPSCITECH.2004.10.005

[52] S.-M. Yuen, C.-C. M. Ma, Y.-Y. Lin, H.-C. Kuan, *Compos. Sci. Technol.* **2007**, *67*, 2564. doi:10.1016/J.COMPSCITECH.2006.12.006

[53] Z. Yang, X. Chen, Y. Pu, L. Zhou, C. Chen, W. Li, L. Xu, B. Yi, Y. Wang, *Polym. Adv. Technol.* **2007**, *18*, 458. doi:10.1002/PAT.885

[54] F. H. Gojny, M. H. G. Wichmann, U. Köpke, B. Fiedler, K. Schulte, *Compos. Sci. Technol.* **2004**, *64*, 2363. doi:10.1016/J.COMPSCITECH.2004.04.002

[55] F. H. Gojny, H. G. Malte, M. H. G. Wichmann, B. Fiedler, K. Schulte, *Compos. Sci. Technol.* **2005**, *65*, 2300. doi:10.1016/J.COMPSCITECH.2005.04.021

[56] C. A. Dyke, M. P. Stewart, J. M. Tour, *J. Am. Chem. Soc.* **2005**, *127*, 4497. doi:10.1021/JA042828H

[57] M. A. Hamon, H. Hu, P. Bhowmik, S. Niyogi, B. Zhao, M. E. Itkis, R. C. Haddon, *Chem. Phys. Lett.* **2001**, *347*, 8. doi:10.1016/S0009-2614(01)01035-1

[58] M. S. P. Shaffer, X. Fan, A. H. Windle, *Carbon* **1998**, *36*, 1603. doi:10.1016/S0008-6223(98)00130-4

[59] J. Chen, A. M. Rao, S. Lyuksyutov, M. E. Itkis, M. A. Hamon, H. Hu, R. W. Cohn, P. C. Eklund, D. T. Colbert, R. E. Smalley, R. C. Haddon, *J. Phys. Chem. B* **2001**, *105*, 2525. doi:10.1021/JP002596I

[60] M. T. Martínez, M. A. Callejas, A. M. Benito, M. Cochet, T. Seeger, A. Ansón, J. Schreiber, C. Gordon, C. Marhic, O. Chauvet, J. L. G. Fierro, W. K. Maser, *Carbon* **2003**, *41*, 2247. doi:10.1016/S0008-6223(03)00250-1

[61] J. E. Riggs, Z. Guo, D. L. Carroll, Y.-P. Sun, *J. Am. Chem. Soc.* **2000**, *122*, 5879. doi:10.1021/JA9942282

[62] M. A. Hamon, J. Chen, H. Hu, Y. S. Chen, M. E. Itkis, A. M. Rao, P. C. Eklund, R. C. Haddon, *Adv. Mater.* **1999**, *11*, 834. doi:10.1002/(SICI)1521-4095(199907)11:10<834::AID-ADMA834>3.0.CO;2-R

[63] F. H. Gojny, M. H. G. Wichmann, B. Fiedler, I. A. Kinloch, W. Bauhofer, A. H. Windle, K. Schulte, *Polymer* **2006**, *47*, 2036. doi:10.1016/J.POLYMER.2006.01.029

[64] A. Peigney, C. Laurent, E. Flahaut, R. R. Bacsa, A. Rousset, *Carbon* **2001**, *39*, 507. doi:10.1016/S0008-6223(00)00155-X

[65] J. A. Kim, D. G. Seong, T. J. Kang, J. R. Youn, *Carbon* **2006**, *44*, 1898. doi:10.1016/J.CARBON.2006.02.026

[66] Y. S. Song, J. R. Youn, *Carbon* **2005**, *43*, 1378. doi:10.1016/J.CARBON.2005.01.007

[67] M. Wong, M. Paramsothy, X. J. Xu, Y. Ren, S. Li, K. Liao, *Polymer* **2003**, *44*, 7757. doi:10.1016/J.POLYMER.2003.10.011

[68] X. Xu, M. M. Thwe, C. Shearwood, K. Liao, *Appl. Phys. Lett.* **2002**, *81*, 2833. doi:10.1063/1.1511532

[69] L. Liu, H. D. Wagner, *Compos. Sci. Technol.* **2005**, *65*, 1861. doi:10.1016/J.COMPSCITECH.2005.04.002

[70] J. B. Bai, *Carbon* **2003**, *41*, 1325. doi:10.1016/S0008-6223(03)00034-4

[71] J. B. Bai, A. Allaoui, *Compos. Part A: Appl. Sci.* **2003**, *34*, 689. doi:10.1016/S1359-835X(03)00140-4

[72] D. Puglia, L. Valentini, J. M. Kenny, *J. Appl. Polym. Sci.* **2003**, *88*, 452. doi:10.1002/APP.11745

[73] H. Miyagawa, L. T. Drzal, *Polymer* **2004**, *45*, 5163. doi:10.1016/J.POLYMER.2004.05.036

[74] C. McClory, T. McNally, G. Brennan, J. Erskine, *J. Appl. Polym. Sci.* **2007**, *105*, 1003. doi:10.1002/APP.26144

[75] F. H. Gojny, K. Schulte, *Compos. Sci. Technol.* **2004**, *64*, 2303. doi:10.1016/J.COMPSCITECH.2004.01.024
[76] D. Zilli, C. Chiliotte, M. M. Escobar, V. Bekeris, G. R. Rubiolo, A. L. Cukierman, S. Goyanes, *Polymer* **2005**, *46*, 6090. doi:10.1016/J.POLYMER.2005.04.086
[77] M. J. Biercuk, M. C. Liaguno, M. Radosavljevic, J. K. Hyun, A. T. Johnson, J. E. Fischer, *Appl. Phys. Lett.* **2002**, *80*, 2767. doi:10.1063/1.1469696
[78] C. A. Martin, J. K. W. Sandler, A. H. Windle, M.-K. Schwarz, W. Bauhofer, K. Schulte, M. S. P. Shaffer, *Polymer* **2005**, *46*, 877. doi:10.1016/J.POLYMER.2004.11.081
[79] E. S. Choi, J. S. Brooks, D. L. Eaton, M. S. Al-Haik, M. Y. Hussaini, H. Garmestani, D. Li, K. Dahmen, *J. Appl. Phys.* **2003**, *94*, 6034. doi:10.1063/1.1616638
[80] X. Jiang, Y. Bin, M. Matsuo, *Polymer* **2005**, *46*, 7418. doi:10.1016/J.POLYMER.2005.05.127
[81] T. Ogasawara, Y. Ishida, T. Ishikawa, R. Yokota, *Compos. Part A: Appl. Sci.* **2004**, *35*, 67. doi:10.1016/J.COMPOSITESA.2003.09.003
[82] S. Barrau, P. Demont, A. Peigney, C. Laurent, C. Lacabanne, *Macromolecules* **2003**, *36*, 5187. doi:10.1021/MA021263B
[83] D. Stauffer, A. Aharony, in *Introduction to Percolation Theory* **1992**, p. 31 (Taylor & Francis: London).
[84] R. Zallen, in *The Physics of Amorphous Solids* **1983** (John Wiley and Sons: New York, NY).
[85] H. M. Kim, K. Kim, S. J. Lee, J. Joo, H. S. Yoon, S. J. Cho, S. C. Lyu, C. J. Lee, *Curr. Appl. Phys.* **2004**, *4*, 577. doi:10.1016/J.CAP.2004.01.022
[86] J.-M. Benoit, B. Corraze, S. Lefrant, W. J. Blau, P. Bernier, O. Chauvet, *Synth. Met.* **2001**, *121*, 1215. doi:10.1016/S0379-6779(00)00838-9
[87] F. Du, J. E. Fischer, K. I. Winey, *J. Polym. Sci., Part B: Polym. Phys.* **2003**, *41*, 3333. doi:10.1002/POLB.10701
[88] K. H. Kim, W. H. Jo, *Compos. Sci. Technol.* **2008**, *68*, 2120. doi:10.1016/J.COMPSCITECH.2008.03.008
[89] P. Bonnet, D. Sireude, B. Garnier, O. Chauvet, *Appl. Phys. Lett.* **2007**, *91*, 201910. doi:10.1063/1.2813625
[90] B. Safadi, R. Andrews, E. A. Grulke, *J. Appl. Polym. Sci.* **2002**, *84*, 2660. doi:10.1002/APP.10436
[91] M. T. Byrne, W. P. McNamee, Y. Gun'ko, *Nanotechnology* **2008**, *19*, 415707. doi:10.1088/0957-4484/19/41/415707
[92] S. L. Ruan, P. Gao, X. G. Yang, T. X. Yu, *Polymer* **2003**, *44*, 5643. doi:10.1016/S0032-3861(03)00628-1
[93] Z. Wang, P. Ciselli, T. Peijis, *Nanotechnology* **2007**, *18*, 455709. doi:10.1088/0957-4484/18/45/455709
[94] K. P. Ryan, M. Cadek, V. Nicolosi, D. Blond, M. Ruether, G. Armstrong, H. Swan, A. Fonseca, J. B. Nagy, W. K. Maser, W. J. Blau, J. N. Coleman, *Compos. Sci. Technol.* **2007**, *67*, 1640. doi:10.1016/J.COMPSCITECH.2006.07.006
[95] C. Bartholome, P. Miaudet, A. Derré, M. Maugey, O. Roubeau, C. Zakri, P. Poulin, *Compos. Sci. Technol.* **2008**, *68*, 2568. doi:10.1016/J.COMPSCITECH.2008.05.021
[96] C. Pan, L.-Q. Ge, Z.-Z. Gu, *Compos. Sci. Technol.* **2007**, *67*, 3271. doi:10.1016/J.COMPSCITECH.2007.03.036
[97] Z. Yang, B. Dong, Y. Huang, L. Liu, F.-Y. Yan, H.-L. Li, *Mater. Lett.* **2005**, *59*, 2128. doi:10.1016/J.MATLET.2005.02.046
[98] Z. Yang, B. Dong, Y. Huang, L. Liu, F.-Y. Yan, H.-L. Li, *Mater. Chem. Phys.* **2005**, *94*, 109. doi:10.1016/J.MATCHEMPHYS.2005.04.029
[99] Z. Jia, Z. Wang, C. Xu, J. Liang, B. Wei, D. Wu, S. Zhu, *Mater. Sci. Eng. A* **1999**, *271*, 395. doi:10.1016/S0921-5093(99)00263-4
[100] C. Velasco-Santos, A. L. Martínez-Hernàndez, F. T. Fisher, R. Ruoff, V. M. Castaño, *Chem. Mater.* **2003**, *15*, 4470. doi:10.1021/CM034243C
[101] S. J. Park, S. T. Kim, M. S. Cho, H. M. Kim, J. Joo, H. J. Choi, *Curr. Appl. Phys.* **2005**, *5*, 302. doi:10.1016/J.CAP.2004.02.013
[102] K. Kim, S. J. Cho, S. T. Kim, I.-J. Chin, H. J. Choi, *Macromolecules* **2005**, *38*, 10623. doi:10.1021/MA051722J
[103] J. Shen, C. Zeng, L. J. Lee, *Polymer* **2005**, *46*, 5218. doi:10.1016/J.POLYMER.2005.04.010
[104] Y. Wang, J. Deng, K. Wang, Q. Zhang, Q. Fu, *J. Appl. Polym. Sci.* **2007**, *104*, 3695. doi:10.1002/APP.25677
[105] S. H. Jin, Y.-B. Park, K. H. Yoon, *Compos. Sci. Technol.* **2007**, *67*, 3434. doi:10.1016/J.COMPSCITECH.2007.03.013
[106] M. R. Karim, C. J. Lee, A. M. S. Chowdhury, N. Nahar, M. S. Lee, *Mater. Lett.* **2007**, *61*, 1688. doi:10.1016/J.MATLET.2006.07.100
[107] H.-X. Wu, R. Tong, X.-Q. Qiu, H.-F. Yang, Y.-H. Lin, R.-F. Cai, S.-X. Qian, *Carbon* **2007**, *45*, 152. doi:10.1016/J.CARBON.2006.07.011
[108] P. Liu, *Eur. Polym. J.* **2005**, *41*, 2693. doi:10.1016/J.EURPOLYMJ.2005.05.017
[109] S. Qin, D. Qin, W. T. Ford, D. E. Resasco, J. E. Herrera, *Macromolecules* **2004**, *37*, 752. doi:10.1021/MA035214Q
[110] M. Liu, T. Zhu, Z. Li, Z. Liu, *J. Phys. Chem.* **2009**, *113*, 9670.
[111] Y.-L. Liu, W.-H. Chen, *Macromolecules* **2007**, *40*, 8881. doi:10.1021/MA071700S
[112] H. Kong, C. Gao, D. Yan, *J. Mater. Chem.* **2004**, *14*, 1401. doi:10.1039/B401180E
[113] A. M. Shanmugharaj, J. H. Bae, R. R. Nayak, S. H. Ryu, *J. Polym. Sci., Part A: Polym. Chem.* **2007**, *45*, 460. doi:10.1002/POLA.21858
[114] C. Gao, C. D. Vo, Y. Z. Jin, W. Li, S. P. Armes, *Macromolecules* **2005**, *38*, 8634. doi:10.1021/MA050823E
[115] Y.-L. Liu, W.-H. Chen, Y.-H. Chang, *Carbohydr. Polym.* **2009**, *76*, 232. doi:10.1016/J.CARBPOL.2008.10.021
[116] Y.-L. Liu, Y.-H. Chang, M. Liang, *Polymer* **2008**, *49*, 5405. doi:10.1016/J.POLYMER.2008.10.015
[117] B. Fragneaud, K. Masenelli-Varlot, A. Gonzalez-Montiel, M. Terrones, J. Y. Cavaillé, *Compos. Sci. Technol.* **2008**, *68*, 3265. doi:10.1016/J.COMPSCITECH.2008.08.013
[118] J. Cui, W.-P. Wang, Y.-Z. You, C. Liu, P. Wang, *Polymer* **2004**, *45*, 8717. doi:10.1016/J.POLYMER.2004.10.068
[119] C.-Y. Hong, Y.-Z. You, C.-Y. Pan, *Polymer* **2006**, *47*, 4300. doi:10.1016/J.POLYMER.2006.04.006
[120] Y.-Z. You, C.-Y. Hong, C.-Y. Pan, *Nanotechnology* **2006**, *17*, 2350. doi:10.1088/0957-4484/17/9/045
[121] Y.-Z. You, C.-Y. Hong, C.-Y. Pan, *Macromol. Rapid Commun.* **2006**, *27*, 2001. doi:10.1002/MARC.200600573
[122] J. Liu, Z. Nie, Y. Gao, A. Adronov, H. Li, *J. Polym. Sci., Part A: Polym. Chem.* **2008**, *46*, 7187. doi:10.1002/POLA.23026
[123] W. Zhou, S. Lv, W. Shi, *Eur. Polym. J.* **2008**, *44*, 587. doi:10.1016/J.EURPOLYMJ.2008.01.020
[124] X. Pei, W. Liu, J. Hao, *J. Polym. Sci., Part A: Polym. Chem.* **2008**, *46*, 3014. doi:10.1002/POLA.22639
[125] G. Xu, Y. Wang, W. Pang, W.-T. Wu, Q. Zhu, P. Wang, *Polym. Int.* **2007**, *56*, 847. doi:10.1002/PI.2212
[126] G. Xu, W.-T. Wu, Y. Wang, W. Pang, Q. Zhu, P. Wang, *Nanotechnology* **2007**, *18*, 145606. doi:10.1088/0957-4484/18/14/145606
[127] G. Xu, W.-T. Wu, Y. Wang, W. Pang, P. Wang, Q. Zhu, F. Lu, *Nanotechnology* **2006**, *17*, 2485.
[128] C.-Y. Hong, Y.-Z. You, C.-Y. Pan, *Chem. Mater.* **2005**, *17*, 2247. doi:10.1021/CM048054L
[129] X. Pei, J. Hao, W. Liu, *J. Phys. Chem. C* **2007**, *111*, 2947. doi:10.1021/JP0673213
[130] M. Weck, J. J. Jackiw, R. R. Rossi, P. S. Weiss, R. H. Grubbs, *J. Am. Chem. Soc.* **1999**, *121*, 4088. doi:10.1021/JA983297Y
[131] C. Slugovc, *Macromol. Rapid Commun.* **2004**, *25*, 1283. doi:10.1002/MARC.200400150
[132] G.-X. Chen, H.-S. Kim, B. H. Park, J.-S. Yoon, *Macromol. Chem. Phys.* **2007**, *208*, 389. doi:10.1002/MACP.200600411
[133] W. Jeong, M. R. Kessler, *Chem. Mater.* **2008**, *20*, 7060. doi:10.1021/CM8020947
[134] W. Jeong, M. R. Kessler, *Carbon* **2009**, *47*, 2406. doi:10.1016/J.CARBON.2009.04.042
[135] Y. Liu, A. Adronov, *Macromolecules* **2004**, *37*, 4755. doi:10.1021/MA0359584
[136] K. R. Yoon, W.-J. Kim, I. S. Choi, *Macromol. Chem. Phys.* **2004**, *205*, 1218. doi:10.1002/MACP.200400077

[137] Z. Jin, K. P. Pramoda, G. Xu, S. H. Goh, *Chem. Phys. Lett.* **2001**, *337*, 43. doi:10.1016/S0009-2614(01)00186-5
[138] R. E. Gorga, R. E. Cohen, *J. Polym. Sci., Part B: Polym. Phys.* **2004**, *42*, 2690. doi:10.1002/POLB.20126
[139] R. Haggenmueller, H. H. Gommans, A. G. Rinzler, J. E. Fischer, K. I. Winey, *Chem. Phys. Lett.* **2000**, *330*, 219. doi:10.1016/S0009-2614(00)01013-7
[140] Z. Zhou, S. Wang, L. Lu, Y. Zhang, Y. Zhang, *Comp. Sci. Technol.* **2007**, *67*, 1861. doi:10.1016/J.COMPSCITECH.2006.10.016
[141] Z. Jin, K. P. Pramoda, S. H. Goh, G. Xu, *Mater. Res. Bull.* **2002**, *37*, 271. doi:10.1016/S0025-5408(01)00775-9
[142] M. Ferrara, H.-C. Neitzert, M. Sarno, G. Gorrasi, D. Sannino, V. Vittoria, P. Ciambelli, *Physica E* **2007**, *37*, 66. doi:10.1016/J.PHYSE.2006.10.008
[143] G. D. Liang, S. C. Tjong, *Mater. Chem. Phys.* **2006**, *100*, 132. doi:10.1016/J.MATCHEMPHYS.2005.12.021
[144] O. Valentino, M. Sarno, N. G. Rainone, M. R. Nobile, P. Ciambelli, H. C. Neitzert, G. P. Simon, *Physica E* **2008**, *40*, 2440. doi:10.1016/J.PHYSE.2008.02.001
[145] M. A. L. Manchado, L. Valentini, J. Biagiotti, J. M. Kenny, *Carbon* **2005**, *43*, 1499. doi:10.1016/J.CARBON.2005.01.031
[146] P. Pötschke, A. R. Bhattacharyya, A. Janke, *Carbon* **2004**, *42*, 965.
[147] S. D. Wanjale, J. P. Jog, *Polymer* **2006**, *47*, 6414. doi:10.1016/J.POLYMER.2006.07.011
[148] E. T. Thostenson, T.-W. Chou, *J. Phys. D: Appl. Phys.* **2002**, *35*, L77. doi:10.1088/0022-3727/35/16/103
[149] F. Du, R. C. Scogna, W. Zhou, S. Brand, J. E. Fischer, K. Winey, *Macromolecules* **2004**, *37*, 9048. doi:10.1021/MA049164G
[150] B. H. Cipriano, A. K. Kota, A. L. Gershon, C. J. Laskowski, T. Kashiwagi, H. A. Bruck, S. R. Raghavan, *Polymer* **2008**, *49*, 4846. doi:10.1016/J.POLYMER.2008.08.057
[151] L. Valentini, J. Biogotti, J. M. Kenny, S. Cantucci, *J. Appl. Polym. Sci.* **2003**, *87*, 708. doi:10.1002/APP.11469
[152] W. E. Dondero, R. E. Gorga, *J. Polym. Sci., Part B: Polym. Phys.* **2006**, *44*, 864. doi:10.1002/POLB.20743
[153] Q. Zhang, S. Rastogi, D. Chen, D. Lippits, P. J. Lemstra, *Carbon* **2006**, *44*, 778. doi:10.1016/J.CARBON.2005.09.039
[154] J. Maultzsch, S. Reich, C. Thomsen, *Phys. Rev. B* **2002**, *65*, 233402. doi:10.1103/PHYSREVB.65.233402
[155] A. Linares, J. C. Canalda, M. E. Cagio, M. C. García-Guitiérrez, A. Nogales, I. Martín-Gullón, J. Vera, T. A. Ezquerra, *Macromolecules* **2008**, *41*, 7090. doi:10.1021/MA801410J
[156] N. Grossiord, P. J. J. Kivit, J. Loos, J. Meuldijk, A. V. Kyrylyuk, P. van der Schoot, C. E. Koning, *Polymer* **2008**, *49*, 2866. doi:10.1016/J.POLYMER.2008.04.033
[157] K. Kobashi, T. Villmow, T. Andres, P. Pötschke, *Sens. Actuators B Chem.* **2008**, *134*, 787. doi:10.1016/J.SNB.2008.06.035
[158] Y. F. Shih, L. S. Chen, R. J. Jeng, *Polymer* **2008**, *49*, 4602. doi:10.1016/J.POLYMER.2008.08.015
[159] F. Deng, T. Ogasawara, N. Takeda, *Compos. Sci. Technol.* **2007**, *67*, 2959. doi:10.1016/J.COMPSCITECH.2007.05.014
[160] M. S. Dresselhaus, G. Dresselhaus, A. Jorio, A. G. Souza Filho, M. A. Pimenta, R. Saito, *Acc. Chem. Res.* **2002**, *35*, 1070. doi:10.1021/AR0101537
[161] Q. Zhao, H. D. Wagner, *Philos. Trans. R. Soc. Lond. A* **2004**, *362*, 2407. doi:10.1098/RSTA.2004.1447
[162] R. J. Nemanich, S. A. Solin, *Phys. Rev. B* **1979**, *20*, 392. doi:10.1103/PHYSREVB.20.392
[163] Y. Huang, R. J. Young, *Carbon* **1995**, *33*, 97. doi:10.1016/0008-6223(94)00109-D
[164] A. Jorio, M. A. Pimenta, A. G. Souza Filho, R. Saito, G. Dresselhaus, M. S. Dresselhaus, *New J. Phys.* **2003**, *5*, 139. doi:10.1088/1367-2630/5/1/139
[165] G. R. Dieckmann, A. B. Dalton, P. A. Johnson, J. Razal, J. Chen, G. M. Giordono, E. Munoz, I. Musselman, R. H. Baughman, R. J. Draper, *J. Am. Chem. Soc.* **2003**, *125*, 1770. doi:10.1021/JA029084X
[166] J. R. Wood, H. D. Wagner, *Appl. Phys. Lett.* **2000**, *76*, 2883. doi:10.1063/1.126505
[167] O. Lourie, H. D. Wagner, *J. Mater. Res.* **1998**, *13*, 2418. doi:10.1557/JMR.1998.0336
[168] S. Reich, H. Jantoljak, C. Thomsen, *Phys. Rev. B* **2000**, *61*, R13389. doi:10.1103/PHYSREVB.61.R13389
[169] J. P. Lu, *Phys. Rev. Lett.* **1997**, *79*, 1297. doi:10.1103/PHYSREVLETT.79.1297
[170] C. A. Cooper, R. J. Young, M. Halsall, *Compos. Part A: Appl. Sci.* **2001**, *32*, 401. doi:10.1016/S1359-835X(00)00107-X
[171] D. F. Farrar, J. Rose, *Biomaterials* **2001**, *22*, 3005. doi:10.1016/S0142-9612(01)00047-3
[172] K. Fuchs, Chr. Friedrich, J. Weese, *Macromolecules* **1996**, *29*, 5893. doi:10.1021/MA951385M
[173] R. Krishnamoorti, E. P. Giannelis, *Macromolecules* **1997**, *30*, 4097. doi:10.1021/MA960550A
[174] M. C. Newstein, H. Wang, N. P. Balsara, A. A. Lefebvre, Y. Shnidman, H. Watanabe, K. Osaki, T. Shikata, H. Niwa, Y. Morishima, *J. Chem. Phys.* **1999**, *111*, 4827. doi:10.1063/1.479245
[175] K. Yurekli, R. Krisnamoorti, M. F. Tse, K. O. McElrath, A. H. Tsou, H. C. Wang, *J. Polym. Sci., Part B: Polym. Phys.* **2001**, *39*, 256. doi:10.1002/1099-0488(20010115)39:2<256::AID-POLB80>3.0.CO;2-Z
[176] K. Lozano, J. Bonilla-Rios, E. V. Barrera, *J. Appl. Polym. Sci.* **2001**, *80*, 1162. doi:10.1002/APP.1200
[177] P. Pötschke, T. D. Fornes, D. R. Paul, *Polymer* **2002**, *43*, 3247. doi:10.1016/S0032-3861(02)00151-9
[178] G. Hu, C. Zhao, S. Zhang, M. Yang, Z. Wang, *Polymer* **2006**, *47*, 480. doi:10.1016/J.POLYMER.2005.11.028
[179] A. K. Kota, B. H. Cipriano, M. K. Duesterberg, A. L. Gershon, D. Powell, S. R. Raghavan, H. A. Bruck, *Macromolecules* **2007**, *40*, 7400. doi:10.1021/MA0711792
[180] M. Castro, J. Lu, S. Bruzaud, B. Kumar, J.-F. Feller, *Carbon* **2009**, *47*, 1930. doi:10.1016/J.CARBON.2009.03.037
[181] K. Kobashi, T. Villmow, T. Andres, P. Pötschke, *Sens. Actuators B Chem.* **2008**, *134*, 787. doi:10.1016/J.SNB.2008.06.035
[182] M. Pumera, A. Merkoçi, S. Alegret, *Sens. Actuators B Chem.* **2006**, *113*, 617. doi:10.1016/J.SNB.2005.07.010
[183] B. Pradhan, R. R. Kohlmeyer, K. Setyowati, H. A. Owen, *Carbon* **2009**, *47*, 1686. doi:10.1016/J.CARBON.2009.02.021
[184] R. H. Baughman, C. Cui, A. A. Zakhidov, Z. Iqbal, J. N. Barisci, G. M. Spinks, G. G. Wallace, A. Mazzoldi, D. De Rossi, A. G. Rinzler, O. Jaschinski, S. Roth, M. Kertesz, *Science* **1999**, *284*, 1340. doi:10.1126/SCIENCE.284.5418.1340
[185] G. M. Spinks, B. Xi, V.-T. Truong, G. G. Wallace, *Synth. Met.* **2005**, *151*, 85. doi:10.1016/J.SYNTHMET.2005.03.006
[186] D. Y. Lee, I.-S. Park, M.-H. Lee, K. J. Kim, S. Heo, *Sens. Actuators A Phys.* **2007**, *133*, 117. doi:10.1016/J.SNA.2006.04.005
[187] B. S. Harrison, A. Atala, *Biomaterials* **2007**, *28*, 344. doi:10.1016/J.BIOMATERIALS.2006.07.044
[188] X. Shi, B. Sitharaman, Q. P. Pham, F. Liang, K. Wu, W. E. Billups, L. J. Wilson, A. G. Mikos, *Biomaterials* **2007**, *28*, 4078. doi:10.1016/J.BIOMATERIALS.2007.05.033
[189] B. Sitharaman, X. Shi, X. F. Walboomers, H. Liao, V. Cuijpers, L. J. Wilson, A. G. Mikos, J. J. Jansen, *Bone* **2008**, *43*, 362. doi:10.1016/J.BONE.2008.04.013
[190] N. A. Kumar, H. S. Ganapathy, J. S. Kim, Y. S. Jeong, Y. T. Jeong, *Eur. Polym. J.* **2008**, *44*, 579. doi:10.1016/J.EURPOLYMJ.2008.09.009
[191] M. Majumder, A. Stinchcomb, B. J. Hinds, *Life Sci.* **2009**, in press. doi:10.1016/J.LFS.2009.04.006
[192] Y.-W. Lee, S. M. Kang, K. R. Yoon, Y. S. Chi, I. S. Choi, S.-P. Hong, B.-C. Yu, H.-J. Paik, W. S. Yun, *Macromol. Res.* **2005**, *13*, 356.
[193] D. Zhou, L. Yang, R. Yang, W. Song, S. Peng, Y. Wang, *Electrophoresis* **2008**, *29*, 4637. doi:10.1002/ELPS.200700925
[194] L. Lacerda, A. Bianco, M. Prato, K. Kostarlos, *Adv. Drug Deliv. Rev.* **2006**, *58*, 1460. doi:10.1016/J.ADDR.2006.09.015
[195] C.-S. Zhang, Q.-Q. Ni, S.-Y. Fu, K. Kurashiki, *Compos. Sci. Technol.* **2007**, *67*, 2973. doi:10.1016/J.COMPSCITECH.2007.05.011
[196] N. G. Sahoo, Y. C. Jung, H. J. Yoo, J. W. Cho, *Compos. Sci. Technol.* **2007**, *67*, 1920. doi:10.1016/J.COMPSCITECH.2006.10.013